Interplay of Collective and Single Particle Modes in the Pairing Properties of Open Shell Nuclei

G. Potel

CEA, Saclay

R.A. Broglia

Milano University and INFN

The Niels Bohr Institute, Copenhagen

A. Idini, E. Vigezzi

INFN Milano

F. Barranco

Sevilla University

INT workshop 8-12 April 2013 - , Seattle

OUTLINE

A. Overview of Mean Field Pairing calculations (HFB)

Including v-14/18 as pairing force

B. PVC and Single-particle self-energy

C. Phonon Exchange Induced Pairing Interaction (Old theory)

D. PVC and Quasi-particle self-energy or SCGF (New theory)

Contact with Ab-Initio approaches to open-shell nuclei

Typical forces employed in finite nuclei pairing HFB-like calculations

I) Monopole: $H_p = - G P^+P$ with G = -25/A MeV

being $P^+ = \Sigma_{m>0} a^+_m a^+_{-m}$; restricted to one shell

ii) Contact interactions $V_c(1-\eta*\rho(r)/\rho_0)$ (E_{cut}=60MeV)

Commonly used with Skyrme forces

iii) Gogny force

Continuum is relevant

iv) Argonne int.

Continuum is crucial

Up to 800MeV

v) Nuclear Matter Calculation Based Pairing Interaction

Show some Illustrative results

Contact interaction

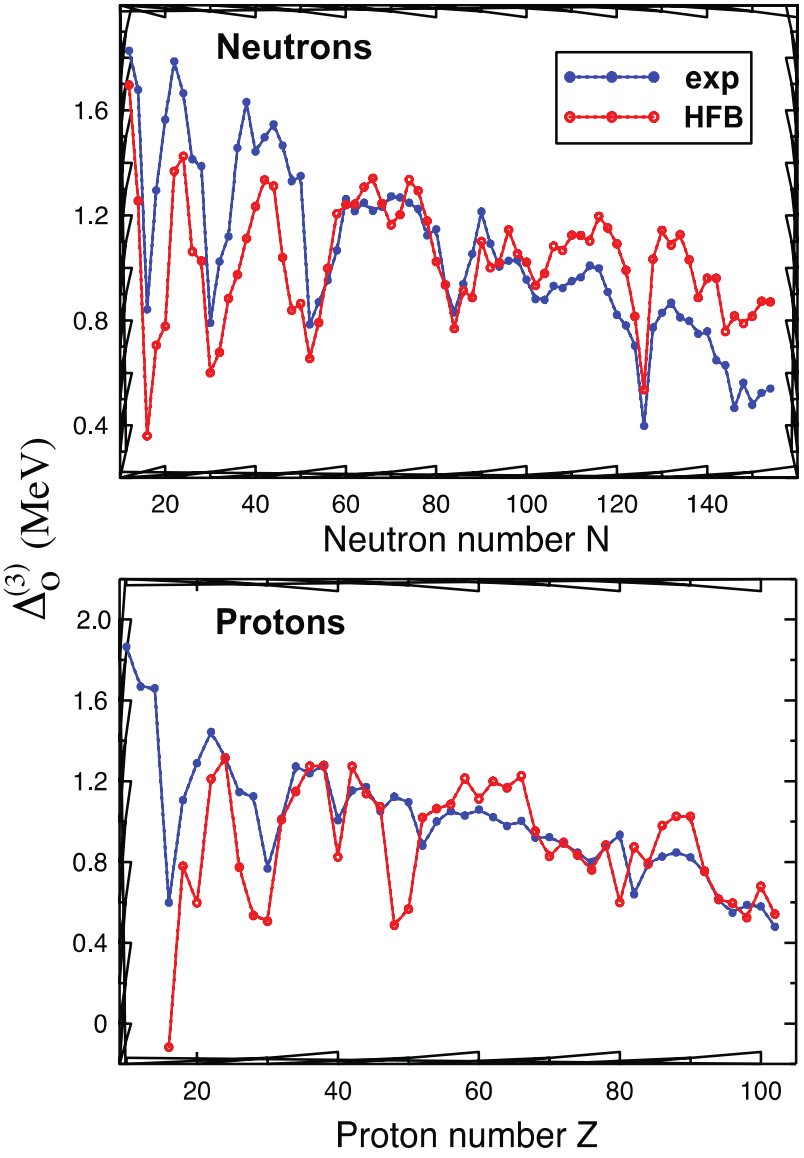

Survey of OES: G.F. Bertsch et al. Phys. Rev. C 79, 034306 (2009)

$$V(r-r') = V_c(1-\eta^*\rho(r)/\rho_0)\ \delta^3(r-r')$$

η=0; 0.5 and 1.0 (vol.; mix.; surf.)

(Ecut=60MeV);

TABLE IV: RMS residuals of $\Delta_o^{(3)}$ obtained in various models. All energies are in MeV. The last column shows the ratio of proton and neutron effective pairing strengths obtained through the optimization procedure. The mass predictions of the HFB-14 model [16] were taken from [51].

Theory	pairing	residual neutrons	residual protons	$V_0^{\rm eff}(p)/V_0^{\rm eff}(n)$
Constant		0.31	0.27	
c/A^α		0.24	0.22	
HF+BCS	volume	0.31	0.38	1.05
HF+BCS	mixed	0.30	0.36	1.08
HF+BCS	surface	0.27	0.35	1.12
HFB	mixed	0.27	0.32	1.11
HFB+LN	mixed	0.23	0.28	1.11
HFB-14		0.46	0.44	1.10

GOGNY GAPS
(Robledo,Bernard,Bertsch,PRC86(2012))

PHYSICAL REVIEW C **86**, 064313 (2012)

Pairing gaps in the Hartree-Fock-Bogoliubov theory with the Gogny D1S interaction

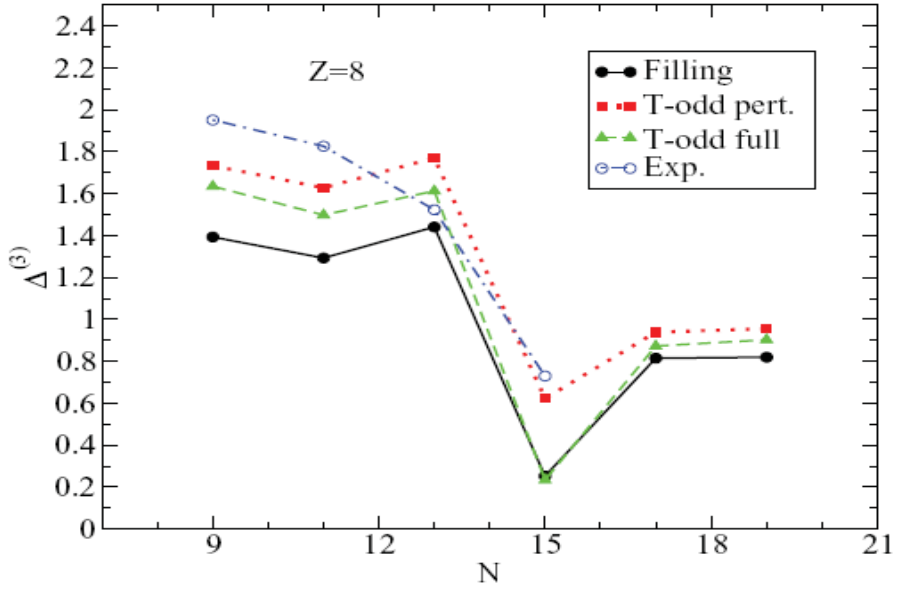

FIG. 1. (Color online) Neutron pairing gaps $\Delta^{(3)}$ in the oxygen isotope chain. Energies were computed in the $N_{sh} = 10$ harmonic oscillator space.

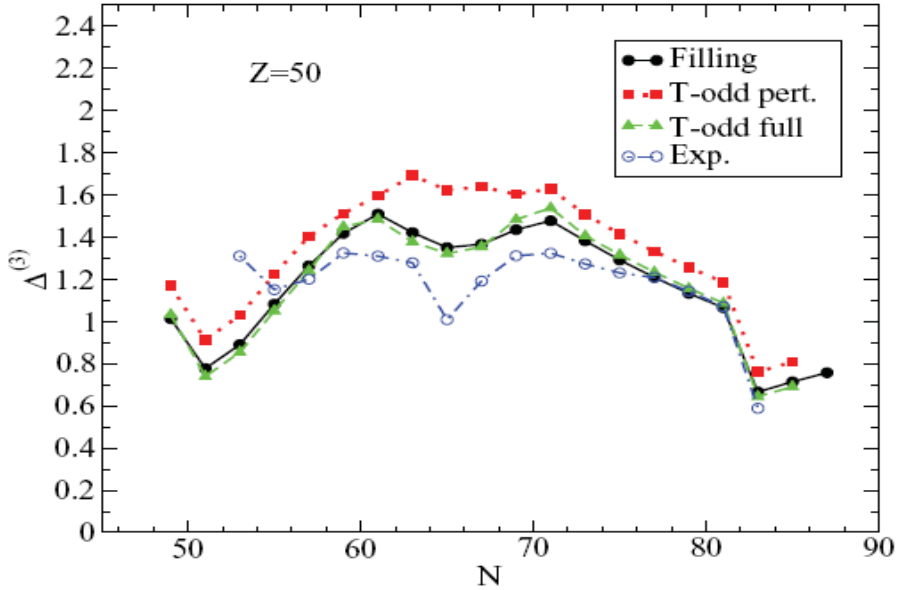

FIG. 2. (Color online) Neutron pairing gaps $\Delta^{(3)}$ in the Sn isotope chain. Energies were computed in the $N_{sh} = 12$ harmonic oscillator space.

GOGNY GAPS (cont.)

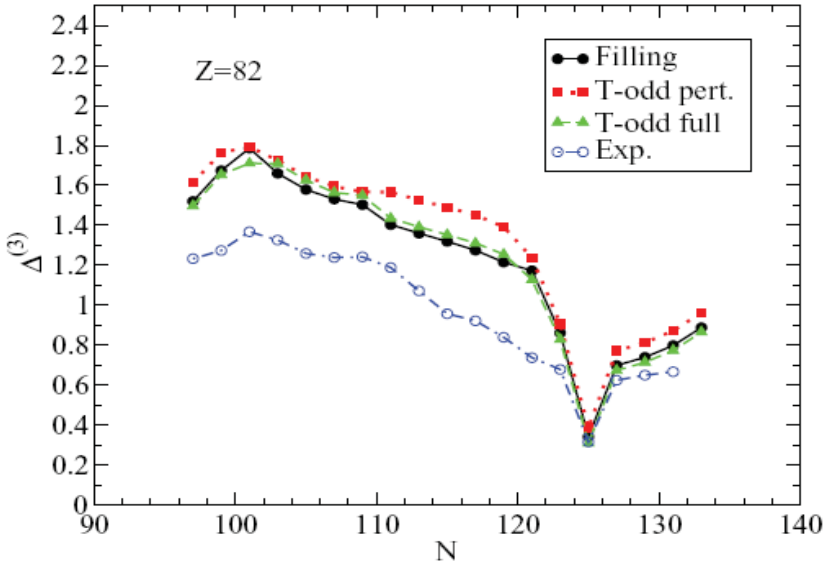

FIG. 3. (Color online) Neutron pairing gaps $\Delta^{(3)}$ in the Pb isotope chain. Energies were computed in the $N_{sh} = 12$ harmonic oscillator space.

Another correlation is associated with the polarization of the nucleus by the valence nucleons. The resulting induced pairing interaction has been calculated to give as strong a contribution as the nucleon-nucleon interaction in the pairing channel [32], Such induced interactions are long-ranged and energy-dependent, and vary from nucleus to nucleus depending on its structure. It would not be surprising that the effects were beyond the scope of the simple energy functionals in current use.

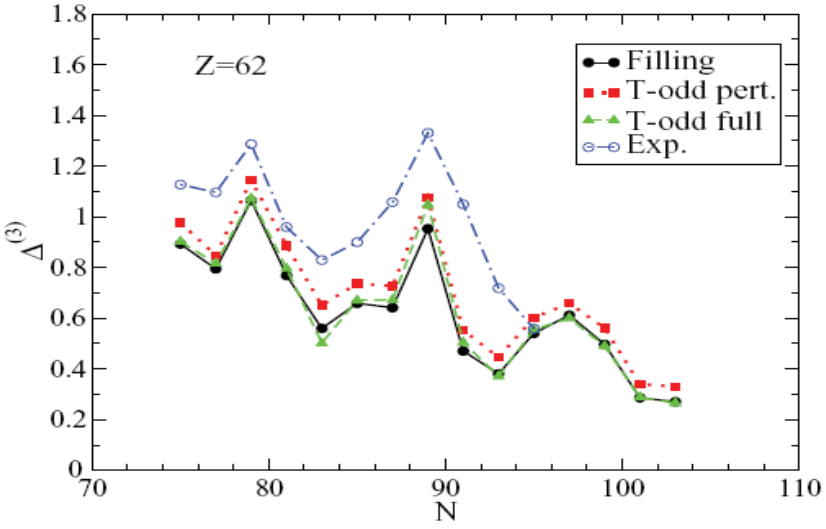

FIG. 4. (Color online) Neutron pairing gaps $\Delta^{(3)}$ in the Sm isotope chain. Energies were computed in the $N_{sh} = 12$ harmonic oscillator space.

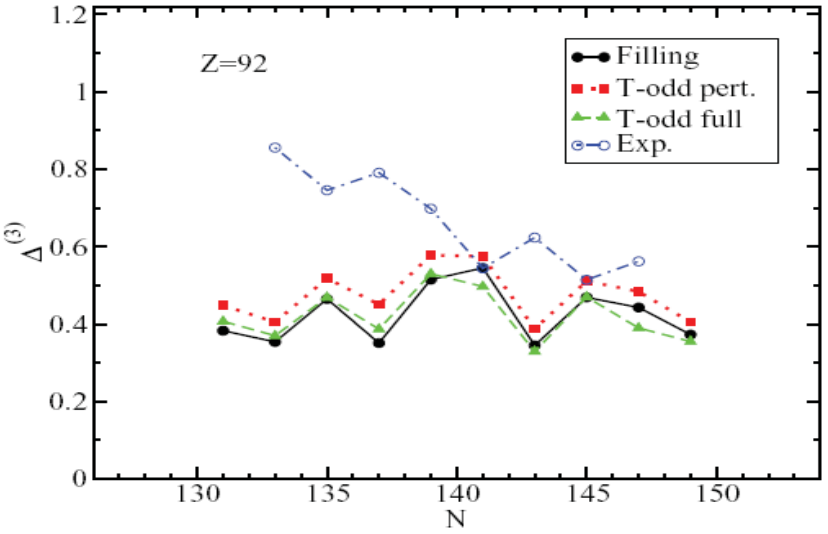

FIG. 5. (Color online) Neutron pairing gaps $\Delta^{(3)}$ in the U isotope chain. Energies were computed in the $N_{sh} = 14$ harmonic oscillator space.

Argonne ($1S_0$)

Barranco, Broglia, Esbensen, Vigezzi, PLB(1997)

Neutron saturated nucleus (Z=50) inmersed in a superfluid neutron sea

We have repeated the calculations, but this time setting the Fermi energy at −7.2 MeV, that is, for the isolated atomic nucleus $^{120}_{50}$Sn. The value of R_{box} has been varied within the range 8–15 fm to check the stability of the results. The values of the pairing gaps become stable once $R_{box} \geqslant 12$ fm. The results of the calculation with R_{box} =15 fm are displayed in Fig. 1(b). The value of the pairing gap at the Fermi energy is $2.2\ ^{+0.4}_{-0.8}$ MeV, the "errors" reflecting the conspicuous state dependence of Δ.[1] This value is about 50% higher than the experimental value of 1.47 MeV deduced from the odd-even mass differences [22]. This also in keeping with the fact that the free nucleon-nucleon interaction seems to provide too strong pairing correlations in finite nuclei (cf. e.g. [23]). In any case, theory provides a sound framework for an eventual quantitative description of pairing in nuclei.

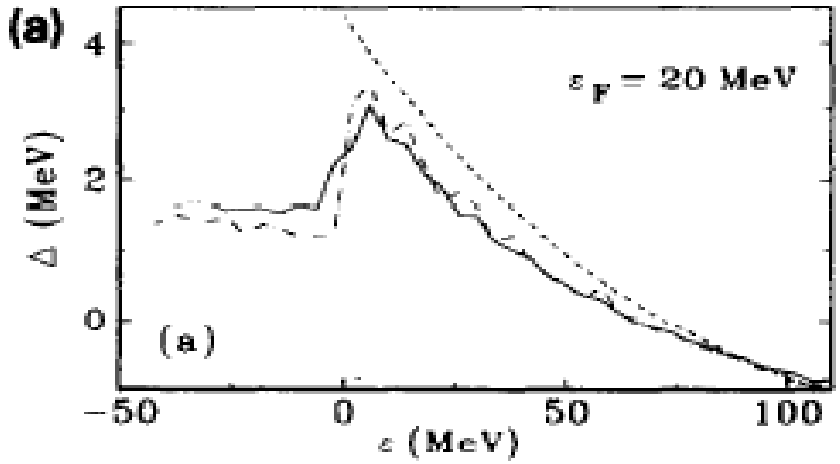

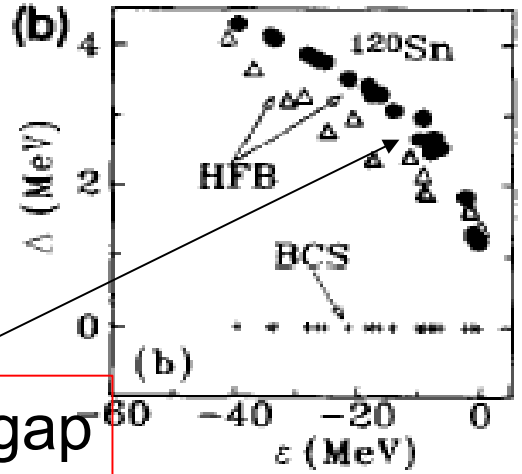

m=1.0 m_0=> Too large gap

Finite size effects on the pairing field (BCS with the bare force)

Potential in the Wigner cell

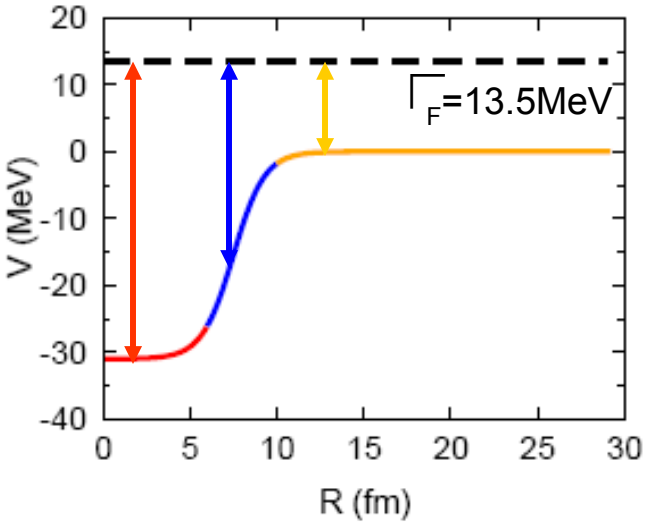

Pairing gap in uniform neutron matter

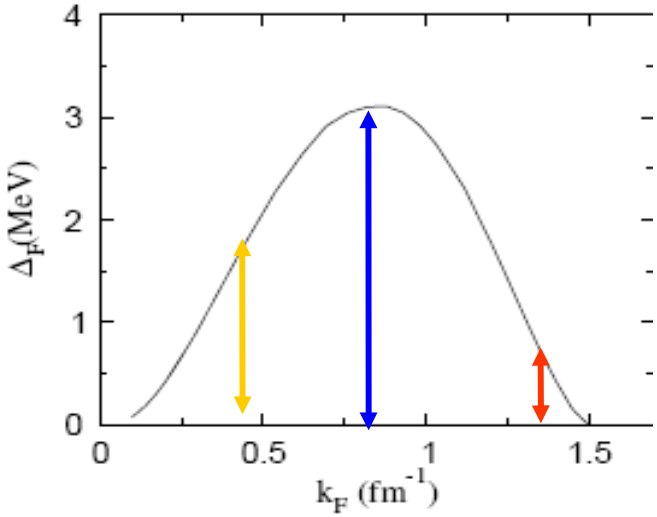

P.M. Pizzochero, F. Barranco, E. Vigezzi, R.A. Broglia,APJ 569(2003)381
N. Sandulescu, Phys. Rev. C70(2004)025801
F. Montani, C. May, H. Muther, PRC 69 (2004) 065801
M. Baldo, U. Lombardo, E.E. Saperstein, S.V. Tolokonnikov, Nucl. Phys. A750 (2005) 409

Spatial dependence of pairing densities and pairing gaps

FINITE NUCLEI, FINITE RANGE FORCE

HFB Equations are expanded on a basis

$$\begin{pmatrix} h_{nn'lj} - \lambda & \Delta_{nn'lj} \\ \Delta_{nn'lj} & -h_{nn'lj} + \lambda \end{pmatrix} \begin{pmatrix} U_{nlj}{}^{\alpha} \\ V_{nlj}{}^{\alpha} \end{pmatrix} = E_{lj}{}^{\alpha} \begin{pmatrix} U_{nlj}{}^{\alpha} \\ V_{nlj}{}^{\alpha} \end{pmatrix}$$

$$\kappa(R_{cm}, r_{12}) = \frac{1}{8\pi} \sum_{nn'lj\alpha} (2j+1)\, U_{nlj}{}^{\alpha *} V_{n'lj}{}^{\alpha} \varphi_{nlj}{}^{*}(r_1)\, \varphi_{n'lj}(r_2)\, P_l(\cos(\vartheta_{12}))$$

$$\Delta(R_{cm}, r_{12}) = -V_{eff}(r_{12}) \kappa(R_{cm}, r_{12})$$

$$\Delta(R_{cm}, k) = \int dr_{12} \Delta(R_{cm}, r_{12}) \;\; \exp(ikr_{12})$$

Spatial description of (non-local) pairing gap
Essential for a consistent description of vortex pinning!

The range of the force is small compared to the coherence length, but not compared to the diffusivity of the nuclear potential

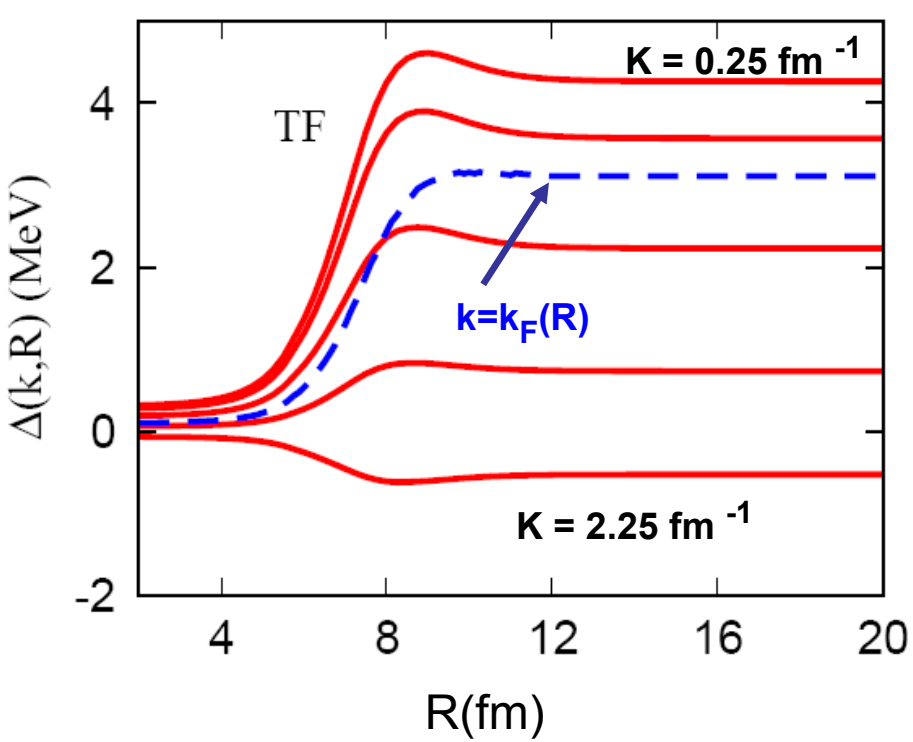

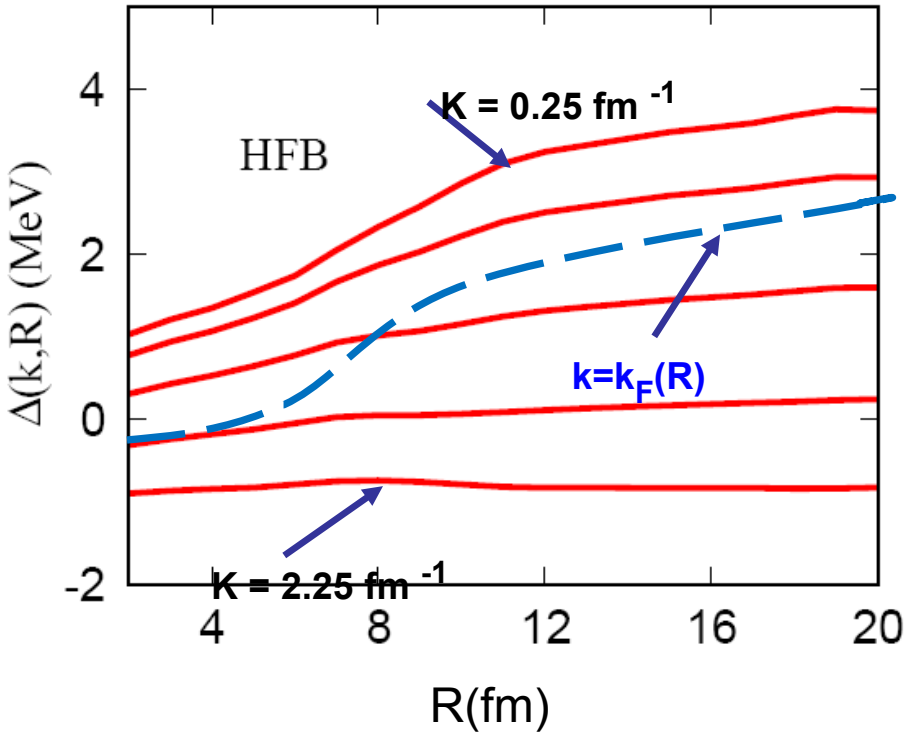

The local-density approximation overstimates the decrease of the pairing gap in the interior of the nucleus. (PROXIMITY EFFECTS)

V_low-k pairing gaps in Sly4 HF field

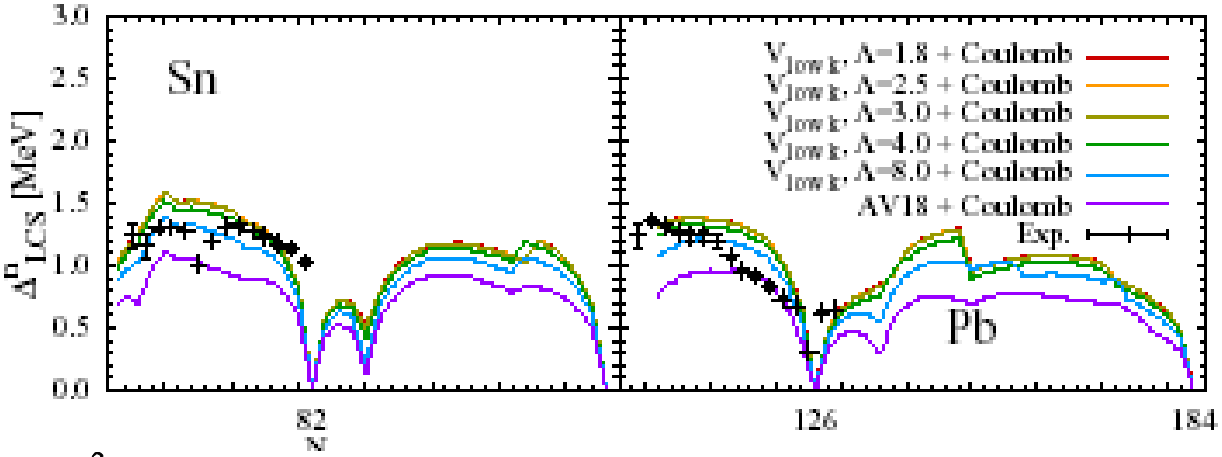

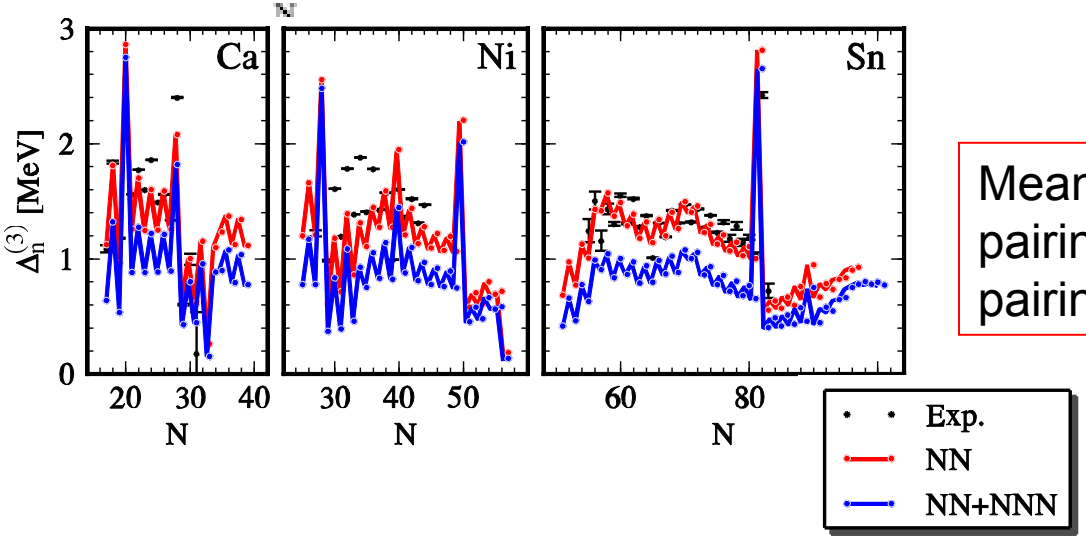

Dependence on the effective mass at high momenta? (Vlow-k vs V18)

Mean field calculation with Vlow-k pairing force: 3-body force reduces the pairing gaps

T. Lesinski,K.Hebeler, T. Duguet, A.Schwenk J.Phys.G39(12)

120Sn with
V_18 and Gogny HF-field: 1.1MeV

Results depend on the Central Potential parameters, including nucleon effective mass.

Any way some solid conclusions can be extracted

1. Bare Argonne is tractable at hfB level

2. With “reasonable” potentials as Sly4 a close to experiment pairing gap is obtained: 1.1MeV vs 1.3MeV.

3. Using V_low-K (and NNN forces)
similar results are obtained

Resonable potential are related to a m*=0.7m_o

which also leave room to ***self-energy corrections (mexp=1.0m0)***

Beyond mean field needed?

a). Neutron matter shows important screening

b). Single-particles are importantly affected, why not quasi-particle properties like the pairing gap?

c). In B&M-II book an estimate was made...

d). If simple DF are used:

(Robledo,Bernard,Bertsch,PRC86(2012))

> Another correlation is associated with the polarization of the nucleus by the valence nucleons. The resulting induced pairing interaction has been calculated to give as strong a contribution as the nucleon-nucleon interaction in the pairing channel [32], Such induced interactions are long-ranged and energy-dependent, and vary from nucleus to nucleus
>
> depending on its structure. It would not be surprising that the effects were beyond the scope of the simple energy functionals in current use.(*)

(*)Alternative sophisticated DF: I. Stetcu (LANL, 2013 talk)

Bohr&Mottelson, Vol.II,1975

6-5f Polarization Contributions to Effective Two-Particle Interactions

In second order, the particle-vibration coupling gives rise to an interaction between two particles, which can be evaluated in a manner similar to the particle-phonon interaction considered in Sec. 6-5d. To illustrate the magnitude of the polarization force, we consider the limiting case in which the frequency of the exchanged phonon is large compared to the energy differences between the particle states. In this case, one can view the interaction as resulting from the static deformation (6-217) produced by the first particle acting on the second. Thus, for a mode of multipolarity λ, one obtains (see Eq. (6-68))

$$V_\lambda(1,2) = -\frac{2\lambda+1}{4\pi C_\lambda} k_\lambda(r_1) k_\lambda(r_2) P_\lambda(\cos\vartheta_{12}) \qquad (6\text{-}228)$$

The order of magnitude of the polarization interaction (6-228) is given by $f_\lambda^2 \hbar\omega_\lambda$ (as for the particle self-energy). For the high-frequency modes, we have $f_\lambda^2 \hbar\omega_\lambda \sim \varepsilon_F A^{-1}$, which is comparable to the average interaction between nucleons in the nucleus ($\sim V_0 A^{-1}$). The magnitude of the polarization interaction can be seen directly from the fact that the deformation of the closed shells produced by a single particle implies polarization moments comparable with the bare moments of the particles (see p. 510); hence, the corresponding contribution to the polarization interaction (6-228) is similar in magnitude to the direct force.

The polarization interaction resulting from the coupling to the low-frequency modes may be considerably larger than the bare force; since the frequencies of these modes may be comparable with the particle frequencies, it may be necessary to go beyond the static approximation (6-228), as in the evaluation of the particle-phonon interaction.

B. Particle Vibration Coupling

and

Single-particle Self-energy

PVC directly related observables

Effective charges

One-particle transfer leading to Vibrational states

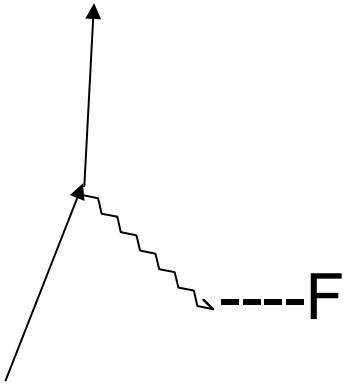

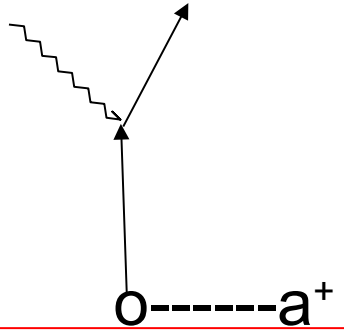

The vertex: Basic Ingredient

hj,j'λ =

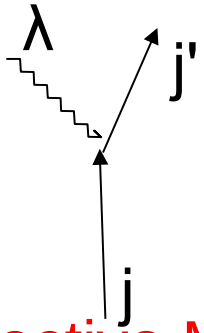

Simple Collective Model value

$$h_{j,j'\lambda} = \beta\lambda(2\lambda+1)^{-1/2}\langle j||R_o\, dU/dr\, Y\lambda||j'\rangle\ (2j+1)^{-1/2}$$

The paradigmatic case; 208Pb(3-) + 1p(h9/2)

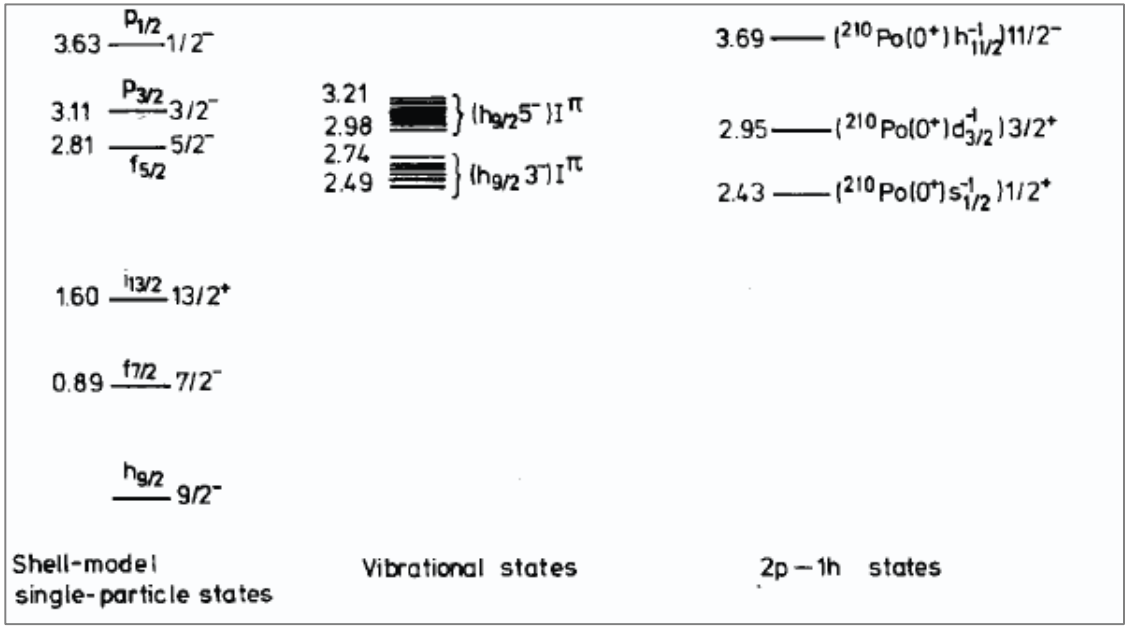

Fig. 11. Observed low-lying energy levels of ^{209}Bi. The coupling of different excitation modes are discussed in the text.

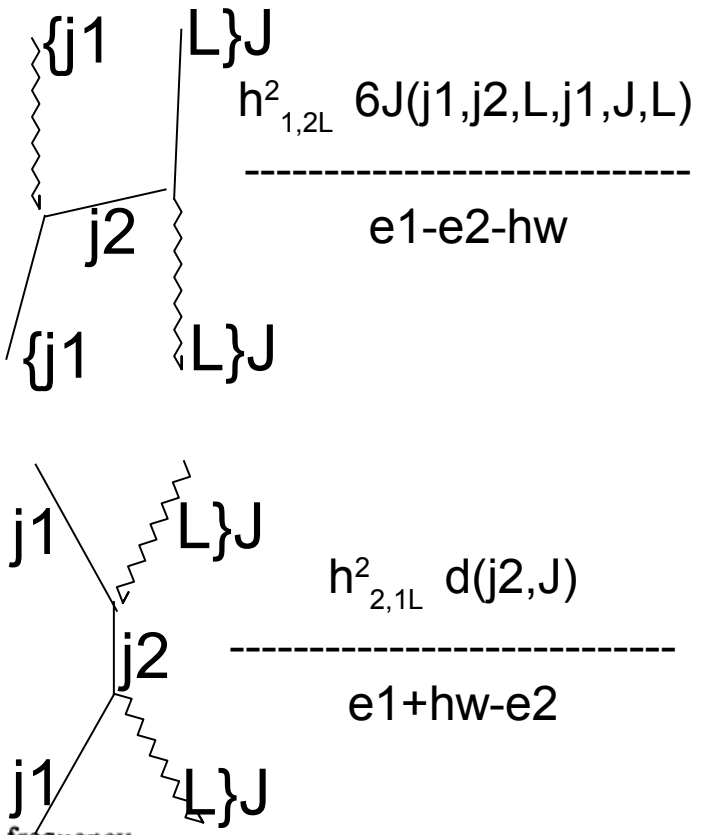

Table 6
Energy shifts of the septuplet members $(h_{9/2}\,3^-)I^\pi$ in ^{209}Bi from the unperturbed vibrational frequency 2.614 MeV. Experimental values are taken from ref. [29]

I	δE_{exp} (keV)	δE_{calc} (keV)
3/2	−120	+36 → −190
5/2	+4	+7
7/2	−29	−6
9/2	−49	−89
11/2	−14	−31
13/2	−14	−63
15/2	+130	+156

I.Hamamoto,1973
Phys.Rep.

SELF ENERGY RENORMALIZATION OF SINGLE-PARTICLE STATES: CLOSED SHELL

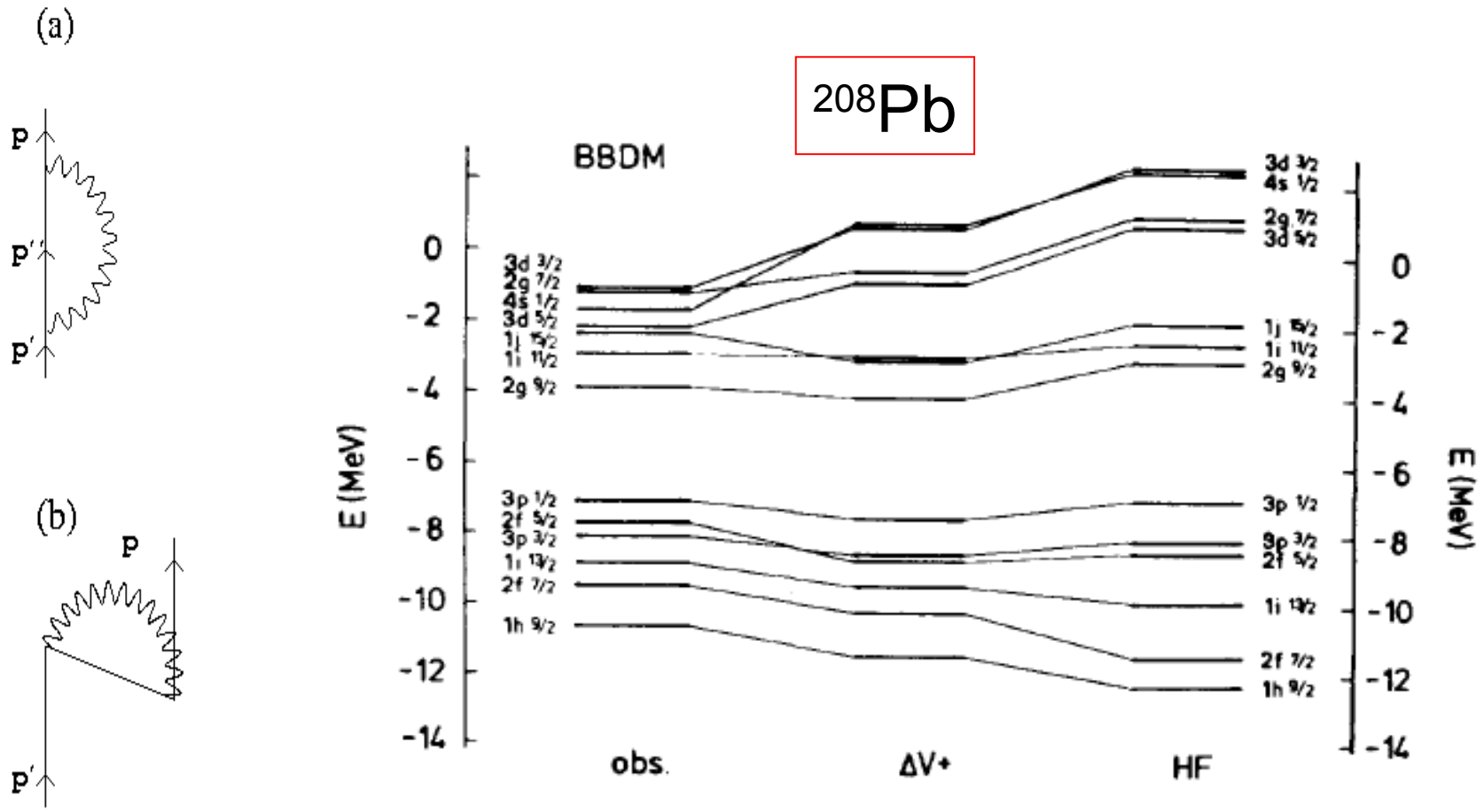

C. Mahaux, P.F. Bortignon, R.A. Broglia, C.H. Dasso and Mahaux, Phys. Rep.(1985)1

Relativistic Mean Field Calculations

Litvinova et al, PRC84, 014305 (2011)

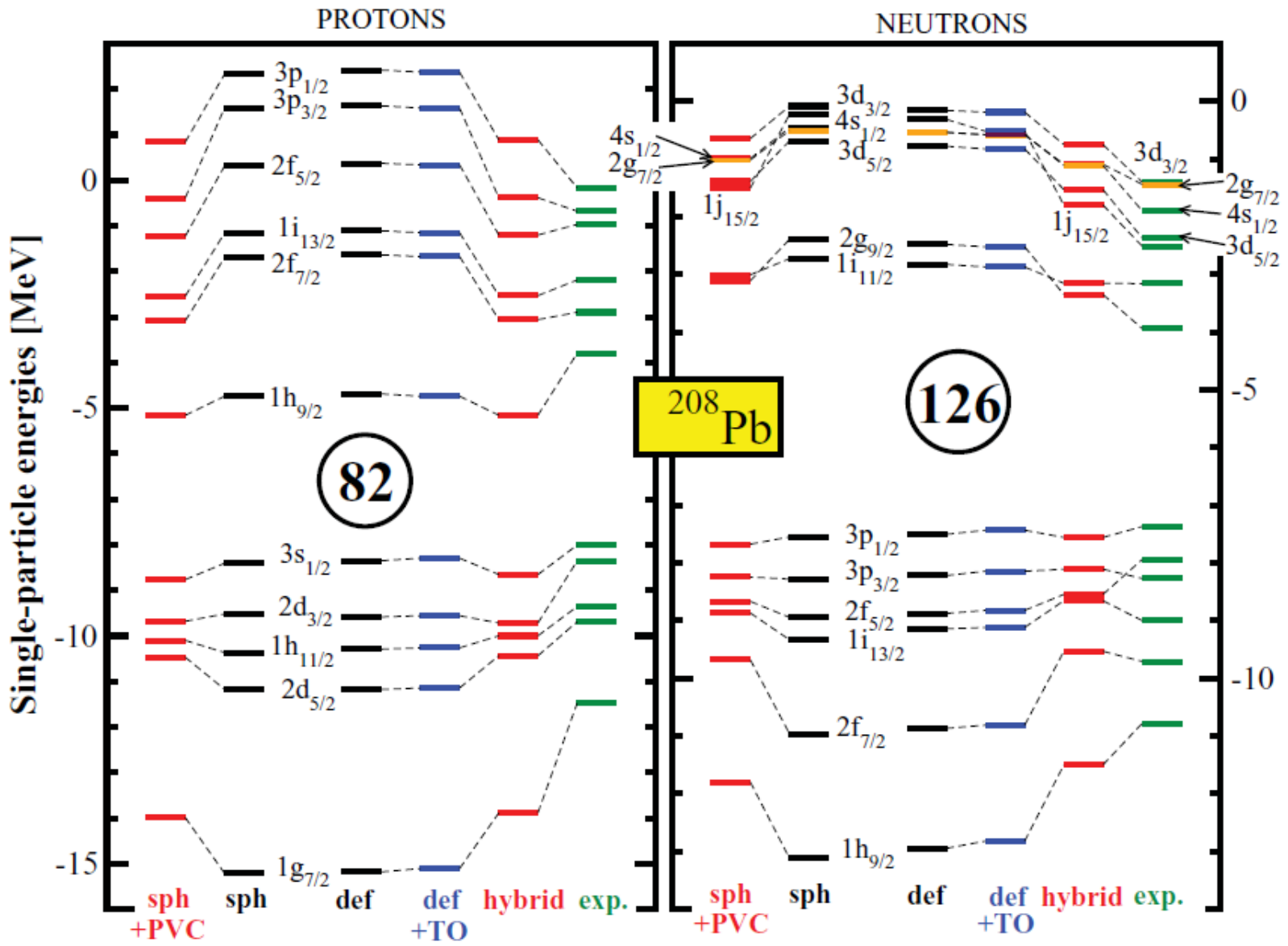

Full Skyrme (Sly5), including momentum dependent terms

Colo' et al, PRC82, 064307

The vertex is deduced from the Transition Densities obtained in RPA calculation

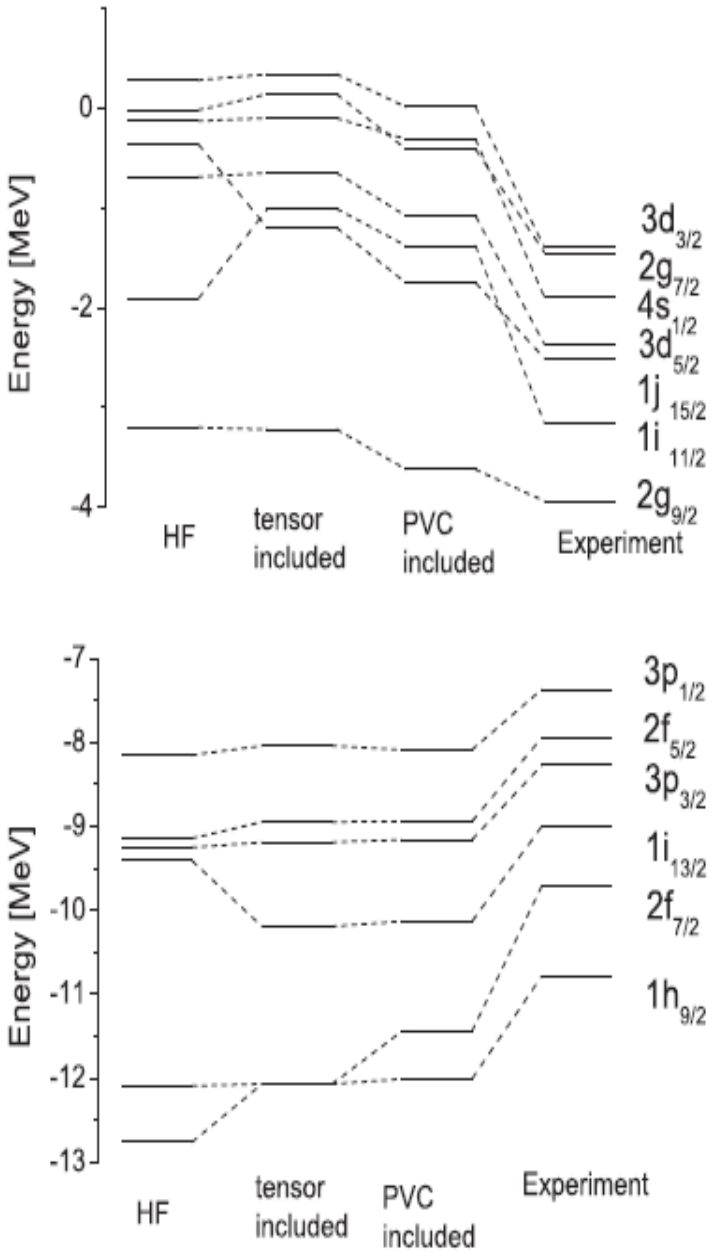

FIG. 6. The same as Fig. 5 for the neutron states in ^{208}Pb.

Similar difficulties in:

Propagation of uncertainties in the Skyrme energy-density-functional model

Y. Gao,[1] J. Dobaczewski,[1,2] M. Kortelainen,[1] J. Toivanen,[1] and D. Tarpanov[2,3]

[1] *Department of Physics, P.O. Box 35 (YFL), FI-40014 University of Jyväskylä, Finland*
[2] *Institute of Theoretical Physics, Faculty of Physics, University of Warsaw, ul. Hoża 69, PL-00-681 Warsaw, Poland*
[3] *Institute for Nuclear Research and Nuclear Energy, 1784 Sofia, Bulgaria*

(Dated: January 28, 2013)

TABLE I: The ^{208}Pb proton (top) and neutron (bottom) s.p. energies $e_{\rm HF}$ (b) and their standard errors (c), as compared to the empirical values (d) [25], residuals, $\Delta(e_{\rm HF}) = e_{\rm HF} - e_{\rm exp}$ (e), PVCs $\delta e_{\rm PVC}$ (f), and residuals of the PVC-corrected s.p. energies $\Delta(e_{\rm PVC}) = e_{\rm HF} + \delta e_{\rm PVC} - e_{\rm exp}$ (g). Where applicable, we also give the root-mean-square (rms) values of entries shown in a given column. All energies are in MeV.

orbital (a)	$e_{\rm HF}$ (b)	$\sigma(e_{\rm HF})$ (c)	$e_{\rm exp}$ (d)	$\Delta(e_{\rm HF})$ (e)	$\delta e_{\rm PVC}$ (f)	$\Delta(e_{\rm PVC})$ (g)
$\pi 3p_{1/2}$	0.219	0.181	−0.16	0.38	−0.440	−0.06
$\pi 3p_{3/2}$	−1.045	0.139	−0.68	−0.37	−0.662	−1.03
$\pi 2f_{5/2}$	−1.284	0.229	−0.97	−0.31	−0.480	−0.79
$\pi 1i_{13/2}$	−2.794	0.238	−2.10	−0.69	−0.221	−0.92
$\pi 1h_{9/2}$	−3.501	0.282	−3.80	0.30	−0.280	0.02
$\pi 2f_{7/2}$	−3.725	0.115	−2.90	−0.83	−0.284	−1.11
$\pi 3s_{1/2}$	−8.036	0.140	−8.01	−0.03	−0.108	−0.13
$\pi 2d_{3/2}$	−8.378	0.199	−8.36	−0.02	0.220	0.20
$\pi 1h_{11/2}$	−9.153	0.207	−9.36	0.21	−0.141	0.07
$\pi 2d_{5/2}$	−10.117	0.117	−9.82	−0.30	0.116	−0.18
$\pi 1g_{7/2}$	−10.908	0.229	−12.00	1.09	0.131	1.22
rms	n.a.	0.196	n.a.	0.52	0.328	0.70
$\nu 3d_{3/2}$	−1.856	0.250	−1.40	−0.46	−0.104	−0.56
$\nu 4s_{1/2}$	−2.051	0.235	−1.90	−0.15	−0.668	−0.82
$\nu 2g_{7/2}$	−2.141	0.258	−1.44	−0.70	−0.280	−0.98
$\nu 1f_{15/2}$	−2.231	0.167	−2.51	0.28	−0.226	0.05
$\nu 3d_{5/2}$	−2.549	0.166	−2.37	−0.18	−0.384	−0.56
$\nu 1i_{11/2}$	−2.680	0.223	−3.16	0.48	−0.271	0.21
$\nu 2g_{9/2}$	−4.336	0.071	−3.94	−0.40	−0.183	−0.58
$\nu 3p_{1/2}$	−7.855	0.109	−7.37	−0.49	0.152	−0.33
$\nu 3p_{3/2}$	−8.503	0.065	−8.26	−0.24	−0.119	−0.36
$\nu 2f_{5/2}$	−8.519	0.143	−7.94	−0.58	0.156	−0.42
$\nu 1i_{13/2}$	−8.603	0.162	−9.24	0.64	−0.130	0.51
$\nu 1h_{9/2}$	−9.922	0.190	−11.40	1.48	0.120	1.60
$\nu 2f_{7/2}$	−10.407	0.103	−9.81	−0.60	0.179	−0.42
rms	n.a.	0.176	n.a.	0.61	0.273	0.68

We will show mainly results obtained using the simple B&MII vertex, based on Experimental beta's

C. Phonon exchange Induced Pairing Interaction (old theory)

Barranco,Broglia,Gori,Vigezzi,Bortignon,Terasaki, PRL11(1999)

$$M^{n}_{\nu,\lambda\nu'} = \frac{\langle \nu' \| R_o \frac{\partial U}{\partial r} Y_\lambda \| \nu \rangle}{\sqrt{2j_\nu + 1}} \frac{\beta_\lambda(n)}{\sqrt{(2\lambda + 1)}} \qquad (1)$$

can be calculated. The quantities entering in the reduced matrix element appearing in Eq. (1) are the nuclear radius R_o, the derivative of the Saxon-Woods potential, and a spherical harmonic of multipolarity λ. Once these matrix elements are known, one can calculate the induced pairing interaction matrix elements (cf. inset of Fig. 1)

$$\upsilon_{\nu\nu'} = \langle (j_{\nu'} m_{\nu'})(j_{\nu'} \tilde{m}_{\nu'}) | v | (j_\nu m_\nu)(j_\nu \tilde{m}_\nu) \rangle_{\text{a.s.}}$$

$$= \sum_{\lambda n} \frac{2}{(2j_{\nu'} + 1)} \frac{2(M^{n}_{\nu,\lambda\nu'})^2}{E_o - [e_\nu + e_{\nu'} + \hbar\omega_\lambda(n)]}, \qquad (2)$$

and thus determine the state dependent BCS pairing gap [2]

$$\Delta_\nu = -\sum_{\nu'} \frac{(2j_{\nu'} + 1)}{2} \frac{\Delta_{\nu'}}{2E_{\nu'}} \upsilon_{\nu\nu'} . \qquad (3)$$

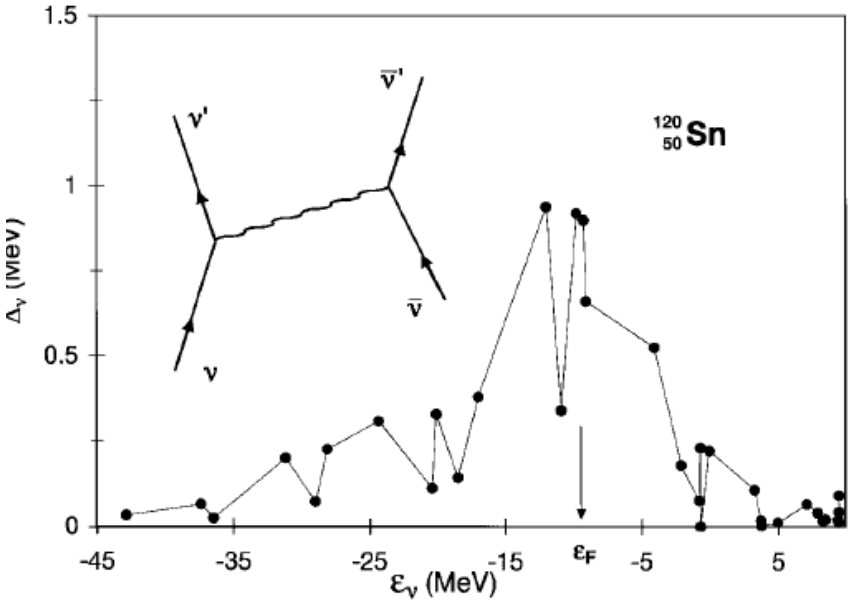

FIG. 1. State dependent pairing gap Δ_ν [cf. Eq. (3)] for the nucleus ^{120}Sn, calculated making use of the induced interaction defined in Eq. (2) (cf. inset, where particles are represented by arrowed lines and phonons by a wavy line).

Comparison between Gogny and Induced Interaction matrix elements

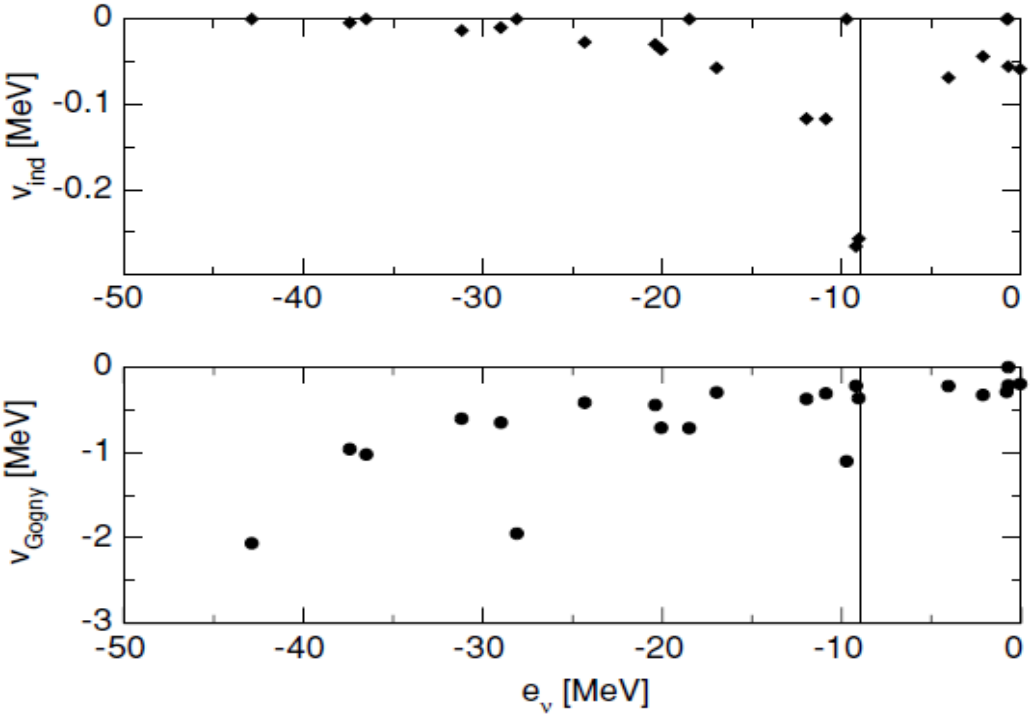

FIG. 1. The nucleus ^{120}Sn. Diagonal pairing matrix elements of the induced interaction (upper panel, solid diamonds) and of the Gogny force (lower panel, solid circles), displayed as a function of the single-particle energy, e_ν, of the state ν calculated using the bare nucleon mass and the single-particle wave functions of a Woods-Saxon potential with standard parameters (depth $V_0 = -49$ MeV, diffusivity $a = 0.65$ fm, and radius $R_0 = 6.16$ fm), including the spin-orbit term, parametrized according to Ref. [21]. Also shown by means of vertical lines is the position of the Fermi energy, $e_F = -9.1$ MeV. Note the different scale in the two figures.

Semiclassical (TF averaged) estimate of diagonal pairing matrix elements in 120Sn.

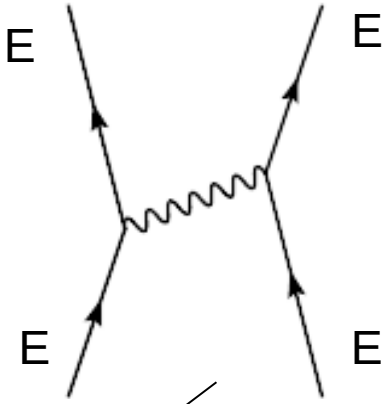

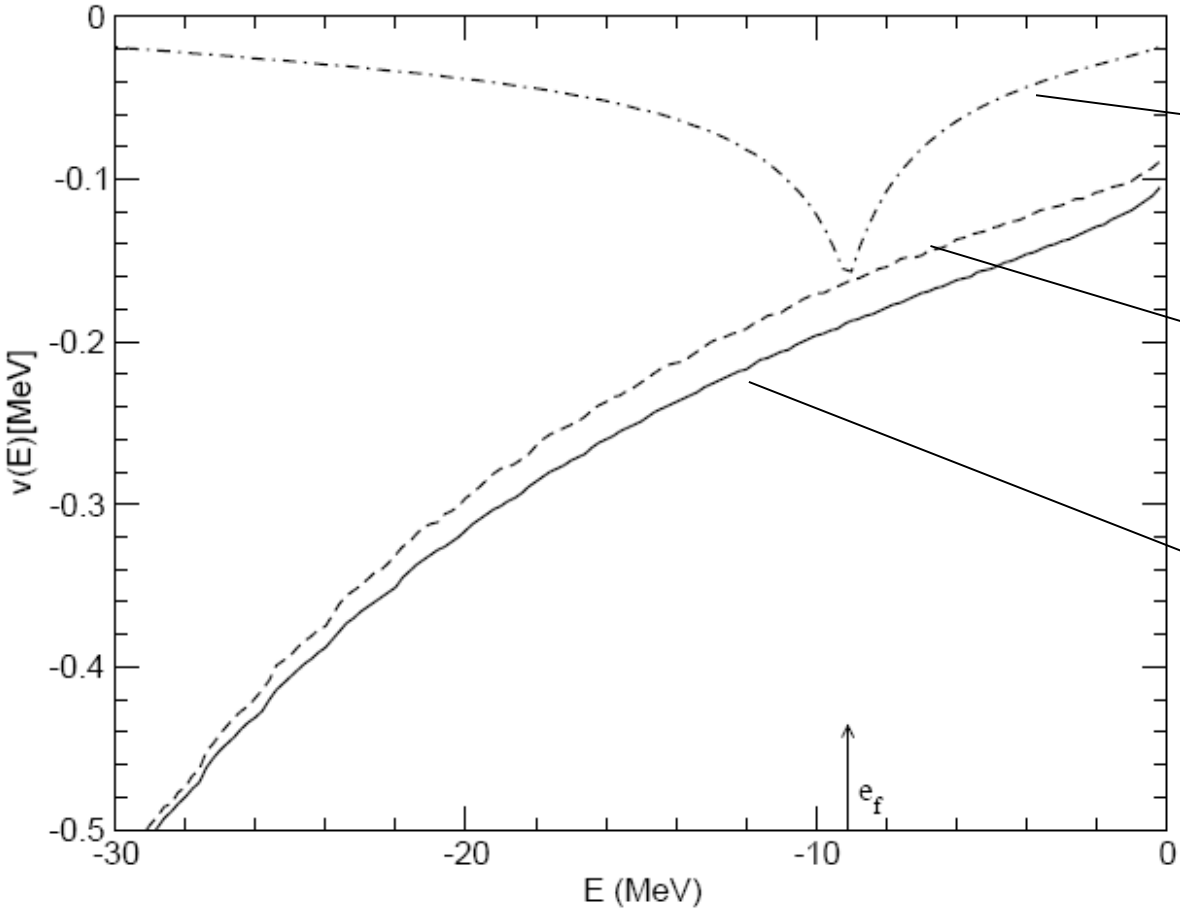

vind

vbare (vlow-k)
L=2fm**-1

vGogny

F. Barranco, P. Schuck et al., Phys. Rev. 72(2005)054314

COMBINING ARGONNE V14 AND INDUCED INTERACTION

The coupling with the phonons induces a surface-peaked interaction and pairing gap

$\Delta \approx Z(v14 + vind)\ \kappa$

A. Pastore et al., PRC 78(2008) 024315

But the pairing density k(r) is much less affected

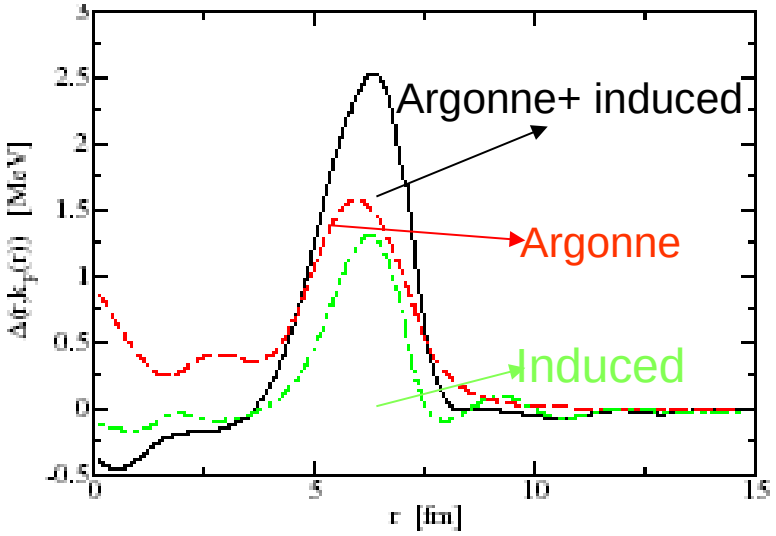

Density modes (surface): Attractive

Spin modes (volume); Repulsive !!

Equivalent DDDI parameters ***Volume Repulsive*** Interaction!!!

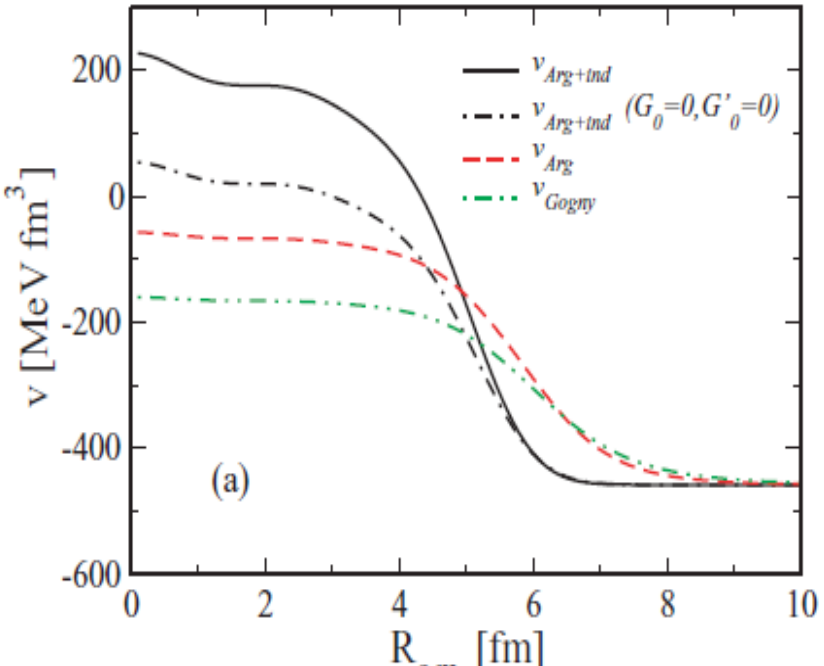

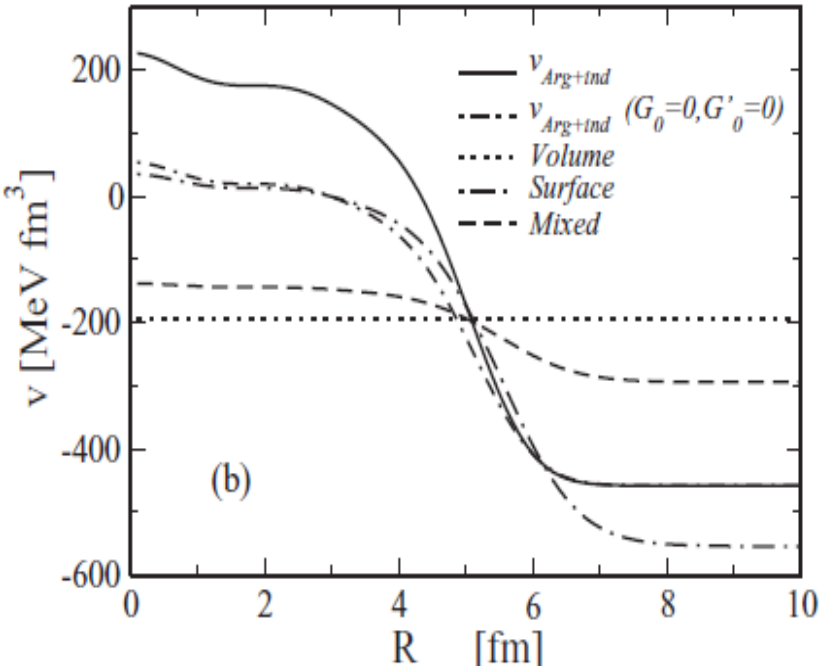

Induced Interaction in the Slab Model (Giovanardi, PRC65,041304(2002)):

Slab Model:Semi-infinte Nuclear Matter with realistic surface statical and dynamical properties (Esbensen&Bertsch Ann.Phys.(1984)

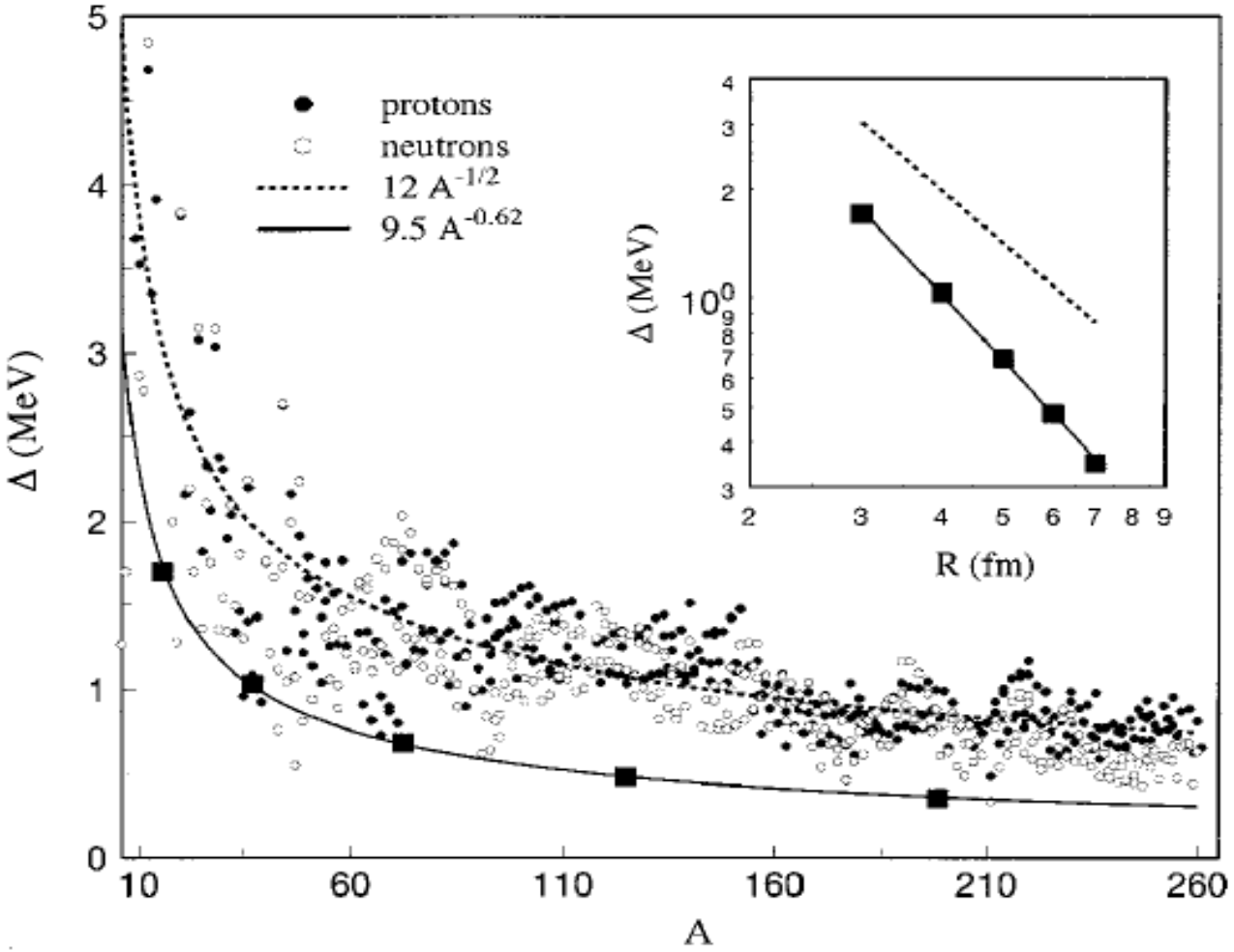

D. Microscopic description of superfluid nuclei beyond mean field:

Quasiparticle Vibration Coupling

(cf. Van der Sluys et al., NPA551(1993)210)

For each single-particle state $a = (q_a n_a l_a j_a)$ the equation-of-motion method leads to a system of linear equations of dimension $2(N+1)$ with N the dimension of the (1qp × phonon) space:

$$\begin{pmatrix} E_a & V(abJ\nu) & 0 & W(abJ\nu) \\ V(abJ\nu) & (E_{J\nu}+E_b) & W(abJ\nu) & 0 \\ 0 & W(abJ\nu) & -E_a & -V(abJ\nu) \\ W(abJ\nu) & 0 & -V(abJ\nu) & -(E_{J\nu}+E_b) \end{pmatrix} \begin{pmatrix} x_0 \\ C_{bJ\nu} \\ -y_0 \\ -D_{bJ\nu} \end{pmatrix} = \tilde{E}_a \begin{pmatrix} x_0 \\ C_{bJ\nu} \\ -y_0 \\ -D_{bJ\nu} \end{pmatrix}. \quad (23)$$

Neglecting the mutual interaction between the (1qp × phonon) states, it becomes easy to rewrite the secular equation (23) as a two-dimensional, hermitian and non-linear eigenvalue problem, by projecting onto the 1qp space:

$$\left[\begin{pmatrix} E_a & 0 \\ 0 & -E_a \end{pmatrix} + \begin{pmatrix} \Sigma_{11}(E) & \Sigma_{12}(E) \\ \Sigma_{12}(E) & \Sigma_{22}(E) \end{pmatrix} \right] \begin{pmatrix} x_0 \\ y_0 \end{pmatrix} = E \begin{pmatrix} x_0 \\ y_0 \end{pmatrix}. \quad (24)$$

The energy-dependent self-energy matrix elements $\Sigma_{ij}(E)$ stand for:

$$\Sigma_{11}(E) = \sum_{bJ\nu} \left(\frac{|V(abJ\nu)|^2}{E-(E_b+E_{J\nu})} + \frac{|W(abJ\nu)|^2}{E+(E_b+E_{J\nu})} \right),$$

$$\Sigma_{22}(E) = \sum_{bJ\nu} \left(\frac{|W(abJ\nu)|^2}{E-(E_b+E_{J\nu})} + \frac{|V(abJ\nu)|^2}{E+(E_b+E_{J\nu})} \right),$$

$$\Sigma_{12}(E) = -\sum_{bJ\nu} V(abJ\nu)\, W(abJ\nu) \left(\frac{1}{E-(E_b+E_{J\nu})} - \frac{1}{E+(E_b+E_{J\nu})} \right). \quad (25)$$

Correcting HFB/BCS Quasiparticles:
2 steps in calculating pairing properties

USED FORMALISM

(Idini, Barranco,Vigezzi,PRC85,014331(2012))

$$\begin{pmatrix} E_a + \Sigma_{11}(\tilde{E}_{a(n)}) & \Sigma_{12}(\tilde{E}_{a(n)}) \\ \Sigma_{12}(\tilde{E}_{a(n)}) & -E_a + \Sigma_{22}(\tilde{E}_{a(n)}) \end{pmatrix} \begin{pmatrix} x_{a(n)} \\ y_{a(n)} \end{pmatrix} = \tilde{E}_{a(n)} \begin{pmatrix} x_{a(n)} \\ y_{a(n)} \end{pmatrix} \quad (10)$$

where one has introduced the normal and abnormal self-energies $\Sigma_{11}(E)$ (being $\Sigma_{22}(E) = -\Sigma_{11}(-E)$) and $\Sigma_{12}(E)$, given by

$$\Sigma_{11} = \sum_{b,m,J,\nu} \frac{V^2(a(n)b(m)J\nu)}{\tilde{E}_{a(n)} - \tilde{E}_{b(m)} - \hbar\omega_{J\nu}} + \sum_{b,m,J,\nu} \frac{W^2(a(n)b(m)J\nu)}{\tilde{E}_{a(n)} + \tilde{E}_{b(m)} + \hbar\omega_{J\nu}} \quad (11)$$

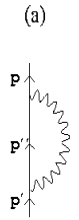

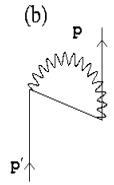

and

$$\Sigma_{12} = \Sigma^{pho}_{12} + \Sigma^{bare}_{12}$$

$$\Sigma^{pho}_{12} = -\sum_{b,m,J,\nu} V(a(n),b(m),J,\nu)W(a(n),b(m),J,\nu) \left[\frac{1}{\tilde{E}_a(n) - \tilde{E}_b(m) - \hbar\omega_{J,\nu}} - \frac{1}{E_a(n) + \tilde{E}_b(m) + \hbar\omega_{J,\nu}}\right].$$

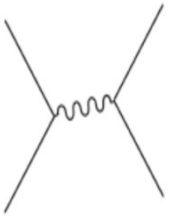

$$\Sigma^{bare}_{12} = \pm \sum_{b,n} V_{bare}(a,b) \frac{(2j_b+1)}{2} \tilde{u}_{b(n)} \tilde{v}_{b(n)}.$$

Optional: 1 or 2 steps?

$V(jj'\lambda) = \beta\lambda(2\lambda+1)^{-1/2}\langle j||Ro\ dU/dr\ Y\lambda||j'\rangle\ (uj\ \tilde{u}j' - vj\ vj')\ (2j+1)^{-1/2}$

$W(jj'\lambda) = \beta\lambda(2\lambda+1)^{-1/2}\langle j||Ro\ dU/dr\ Y\lambda||j'\rangle\ (uj\ vj' + vj\ \tilde{u}j')\ (2j+1)^{-1/2}$

BCS-like rewriting

$$\begin{pmatrix} (\epsilon_{a(n)}-e_F)+\Sigma_{11}(a,E_{a(n)}) & \Sigma_{12}(a,E_{a(n)}) \\ \Sigma_{12}(a,E_{a(n)}) & -(\epsilon_{a(n)}-e_F)+\Sigma_{22}(a,E_{a(n)}) \end{pmatrix} \begin{pmatrix} u_{a(n)} \\ v_{a(n)} \end{pmatrix} = E_{a(n)} \begin{pmatrix} u_{a(n)} \\ v_{a(n)} \end{pmatrix}$$

multiply by $Z_{a(n)}=\left(1-\frac{\Sigma_{odd}(a,E_{a(n)})}{E_{a(n)}}\right)^{-1}$

$$\begin{pmatrix} (e_{a(n)}-e_F) & \Delta(a,E_{a(n)}) \\ \Delta(a,E_{a(n)}) & -(e_{a(n)}-e_F) \end{pmatrix} \begin{pmatrix} u_{a(n)} \\ v_{a(n)} \end{pmatrix} = E_{a(n)} \begin{pmatrix} u_{a(n)} \\ v_{a(n)} \end{pmatrix}$$

new single-particle energies

$$e_{a(n)}-e_F=Z_{a(n)}[(\epsilon_a-e_F)+\Sigma_{even}(a,E_{a(n)})]$$

effective gap

$$\Delta_{a(n)}=Z_{a(n)}(\Sigma_{12}^{bare}+\Sigma_{12}^{pho})\equiv\frac{2E_{a(n)}u_{a(n)}v_{a(n)}}{u_{a(n)}^2+v_{a(n)}^2}$$

where

$$\begin{cases} \Sigma_{odd}(a,E_{a(n)})=\dfrac{\Sigma_{11}(a,E_{a(n)})-\Sigma_{11}(a,-E_{a(n)})}{2} \\ \Sigma_{even}(a,E_{a(n)})=\dfrac{\Sigma_{11}(a,E_{a(n)})+\Sigma_{11}(a,-E_{a(n)})}{2} \end{cases}$$

Since self-energies are energy dependent many solutions are obtained: n=1,2,..
Each carrying a quasi-particle strength $u(a,n)^2+v(a,n)^2<1$
Closure requires Σ_n $u(a,n)^2+v(a,n)^2=1$

A generalized gap equation. Different versions

Expressing u*v as a function of sigma12, and reintroducing them in the sigma12 expression, a close expression for sigma is obtained

$$\Delta_{a(n)} = -Z_{a(n)} \sum_{b(m)} V_{eff}(a(n),b(m)) N_{b(m)} \frac{\Sigma_{12}(b(m),E_{b(m)})}{2\sqrt{(\epsilon_b - e_F + \Sigma_{even}(b(m),E_{b(m)}))^2 + \Sigma_{12}^2(b(m),E_{b(m)})}}$$

c.f.Baldo

where N is the proper quasi-particle normalization:

$$N_{b(m)} = \tilde{u}_{b(m)}^2 + \tilde{v}_{b(m)}^2 = \left(1 - \frac{\partial \Sigma_{11}(a,E_{a(n)})}{\partial E_{a(n)}} u_{b(m)}^2 - \frac{\partial \Sigma_{22}(a,E_{a(n)})}{\partial E_{a(n)}} v_{b(m)}^2 - 2\frac{\partial \Sigma_{12}(a,E_{a(n)})}{\partial E_{a(n)}} u_{b(m)} v_{b(m)}\right)^{-1} < 1$$

which gives the properly normalized u,v's starting from the normalized to 1 u,v's,

and where the effective interaction is

$$V_{eff}(a(n),b(m)) = V_{bare}(a,b) + \sum_{J,\nu} h^2(a,b,J,\nu)\left(\frac{1}{E_{an} - E_{bm} - \hbar\omega_{J,\nu}} - \frac{1}{E_{an} + E_{bm} + \hbar\omega_{J,\nu}}\right)$$

Reintroducing the Zb-factor

$$\Delta_{a(n)} = -Z_{a(n)} \sum_{b(m)} V_{eff}(a(n),b(m)) N_{b(m)} \frac{Z_{b(m)} \Sigma_{12}(b(m),E_{b(m)})}{2\sqrt{Z_{b(m)}^2 (\epsilon_b - e_F + \Sigma_{even}(b(m),E_{b(m)}))^2 + Z_{b(m)}^2 \Sigma_{12}^2(b(m),E_{b(m)})}}$$

$$\Delta_{a(n)} = -\sum_{b(m)} V_{eff}(a(n),b(m)) \frac{Z_{a(n)} \Delta_{b(m)} N_{b(m)}}{2\sqrt{(e_b - e_F)^2 + \Delta_{b(m)}^2}}$$

$$\Delta_{a(n)} = -\sum_{b(m)} V_{eff}(a(n),b(m)) \frac{Z_{a(n)} \Delta_{b(m)} N_{b(m)}}{2E_{b(m)}}$$

Generalized Gap Equation (schematic)

Z=1 free Fermi gas

Z<1 correlated Fermi system

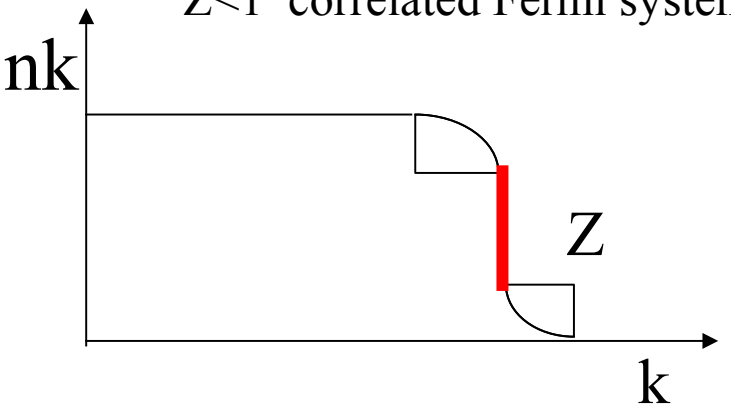

Quasiparticle strength <1

Bare+Induced interaction

$$\Delta_p = -\frac{1}{2}\int d^3p' \frac{Z_p V_{pp'} Z_{p'}}{\sqrt{(\tilde{\varepsilon}_{p'} - \varepsilon_F)^2 + \Delta_{p'}^2}} \Delta_{p'}$$

Renormalized s.p. energy

RENORMALIZING Argonne (on Sly4) pairing gaps (2 steps calculation)

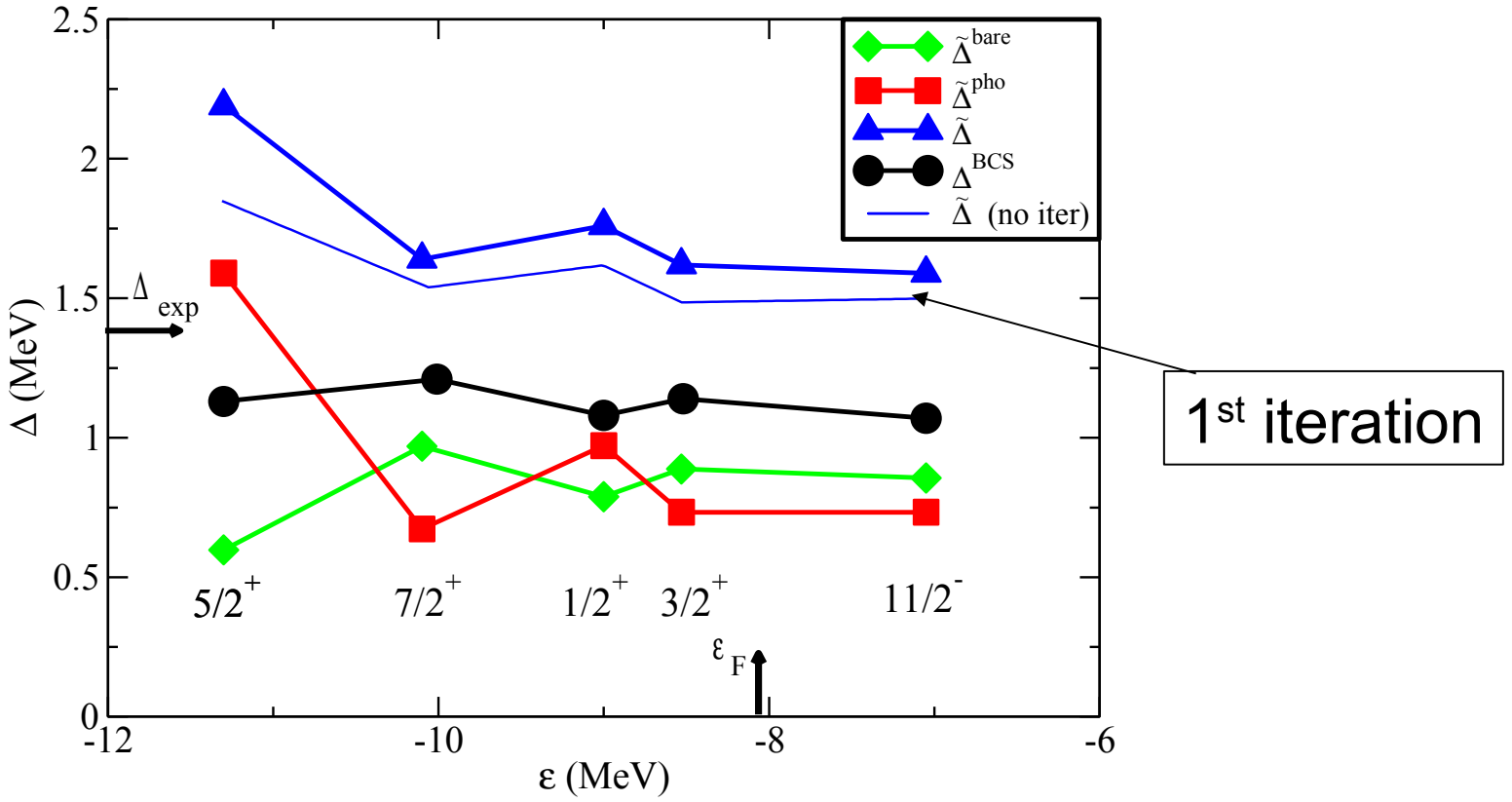

Experimental phonons were used for the density modes L=2,3,4,5
Spin modes not included in this results

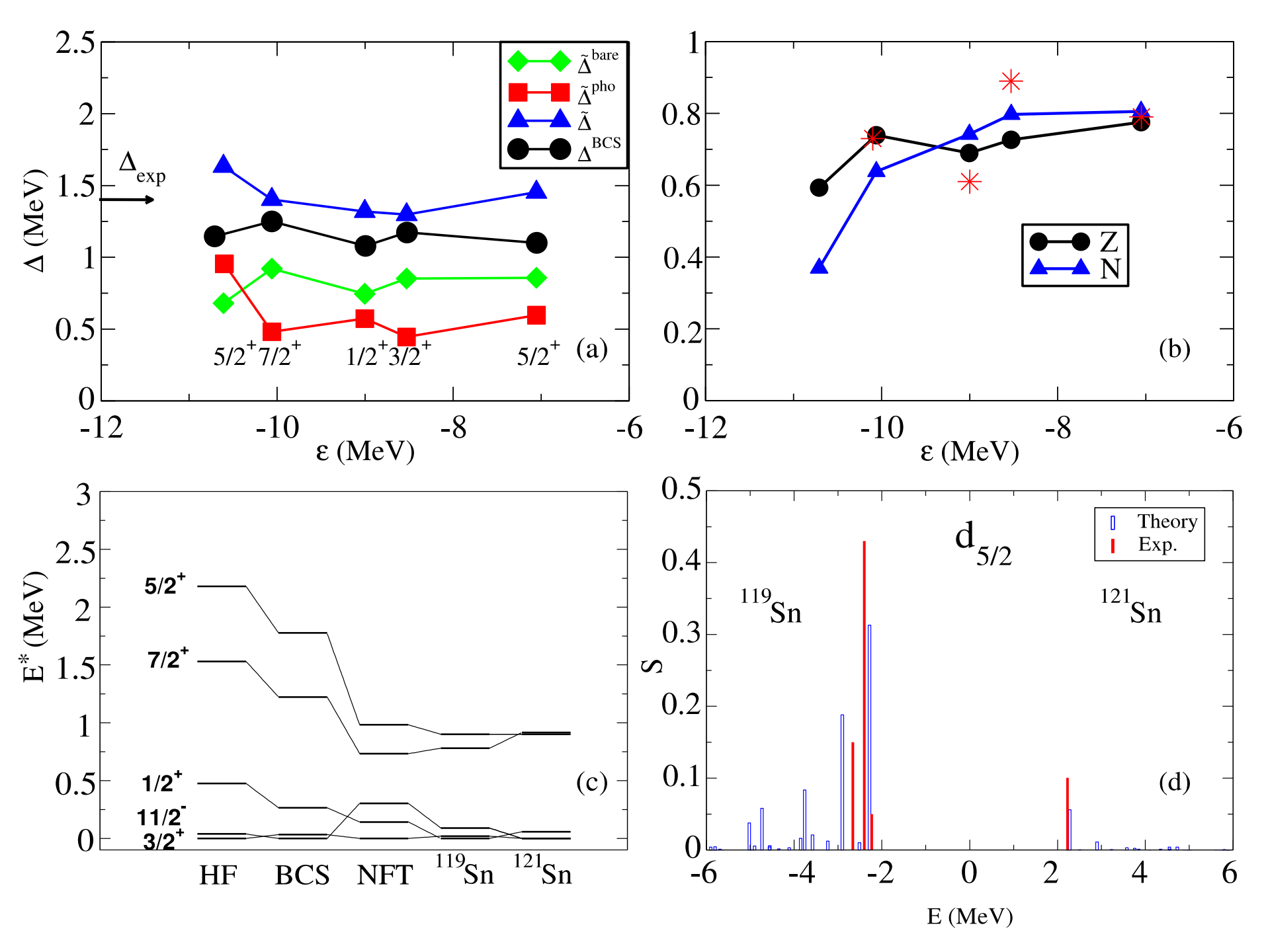
Δ (MeV)
ε (MeV)
$\tilde{\Delta}^{bare}$
$\tilde{\Delta}^{pho}$
$\tilde{\Delta}$
Δ^{BCS}
Δ_{exp}
5/2+ 7/2+
1/2+ 3/2+
5/2+
(a)
(b)
Z
N
E* (MeV)
5/2+
7/2+
1/2+
11/2-
3/2+
HF
BCS
NFT
119Sn
121Sn
(c)
S
E (MeV)
Theory
Exp.
d5/2
119Sn
121Sn
(d)

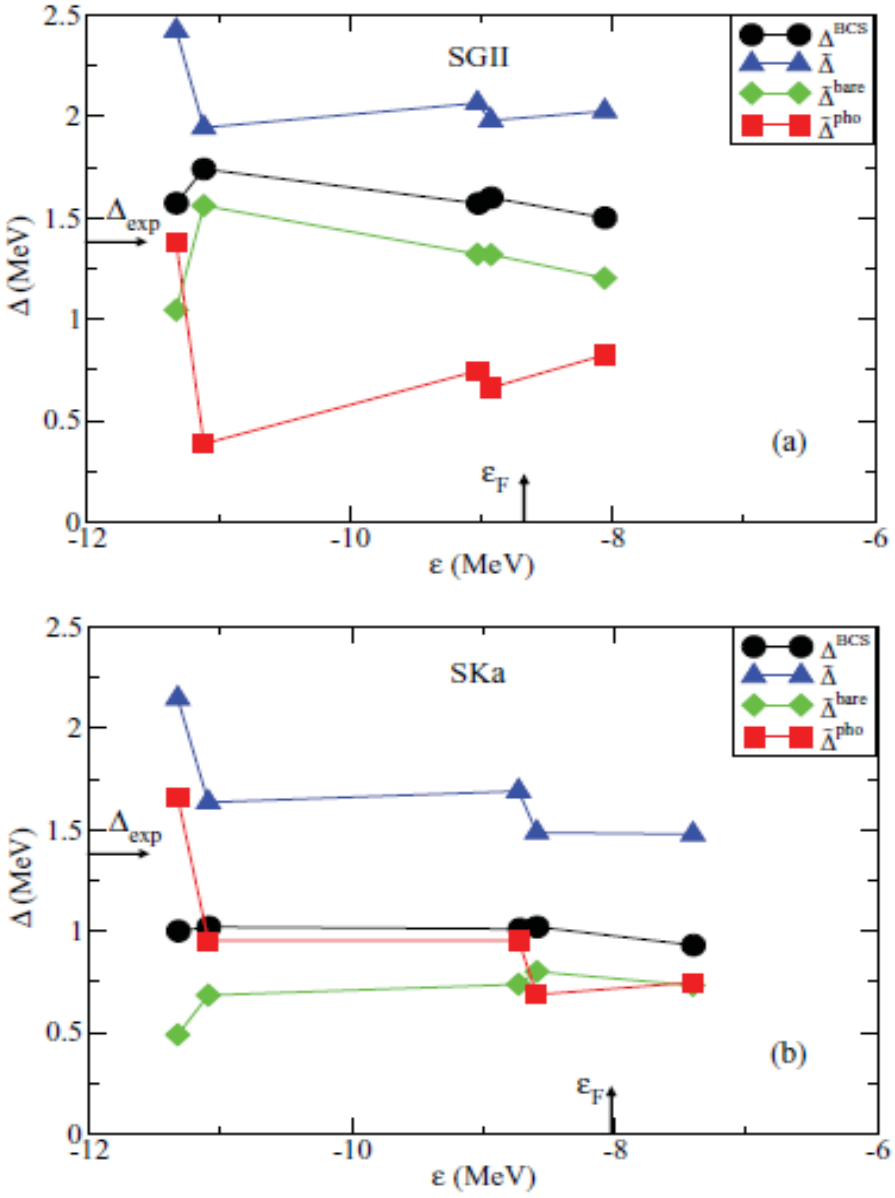

FIG. 17. (Color online) The state-dependent pairing gap Δ^{BCS} calculated in BCS with the bare v_{14} interaction is compared to the renormalized gap $\tilde{\Delta}$ [cf. Eq. (38)] obtained solving the Nambu-Gor'kov equations. We compare results obtained with a mean field

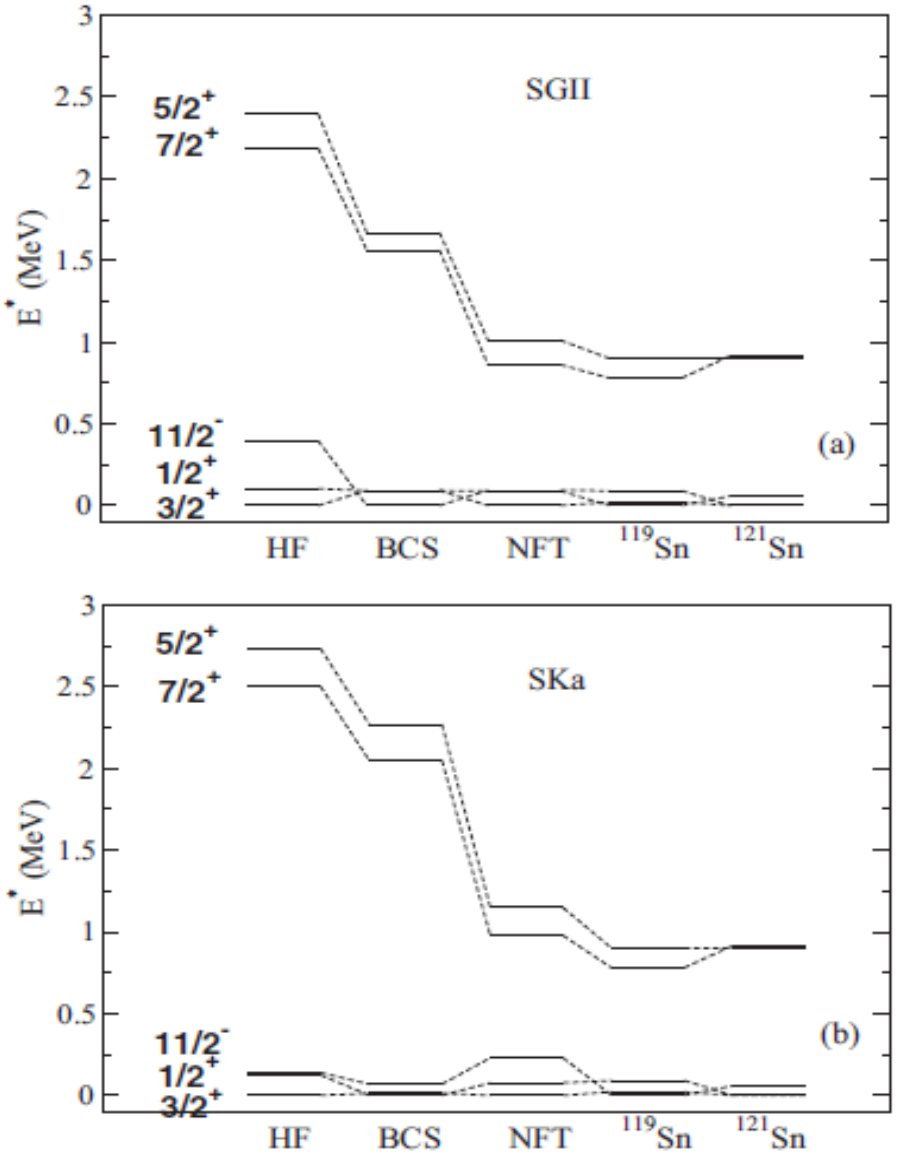

FIG. 18. The theoretical quasiparticle spectra obtained at the various steps of the calculation are compared to the experimental data. We compare results obtained with a mean field produced with the SGII interaction (a) and with the SKa interaction (b) (cf. Fig. 8 for the corresponding calculation with the SLy4 mean field).

Compare 1 and 2 step calculations
Using a simple monopole pairing force

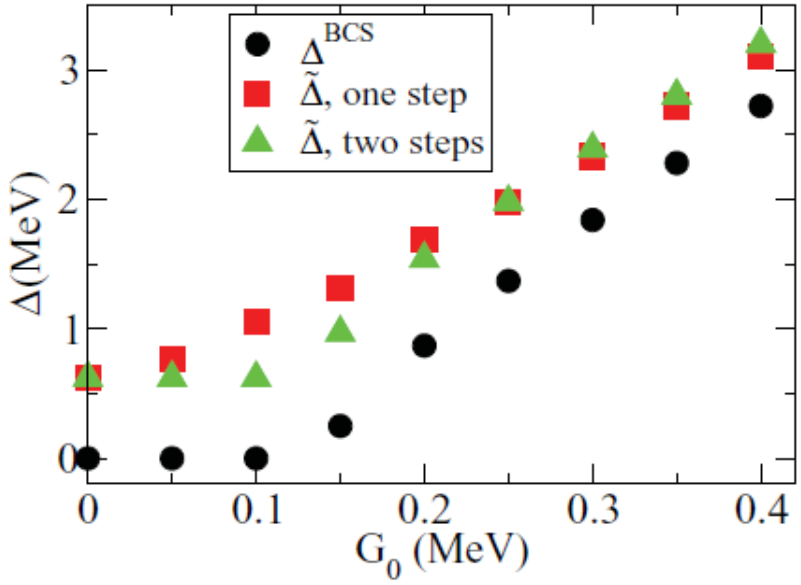

FIG. 26. (Color online) Renormalized gaps $\tilde{\Delta}$ obtained solving the Nambu Gor'kov equations in the one-step and the two-steps diagonalization schemes with the monopole pairing force as a function of the pairing constant G_0, averaged over the five valence orbitals. Also shown is the gap Δ^{BCS} obtained solving the BCS equation.

Full basis formulation,
A.Idini,Ph.D. Thesis,Milano 2013

Allows correcting r-dependence

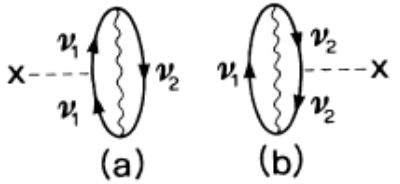

Barranco,Broglia,PRL29(1987)

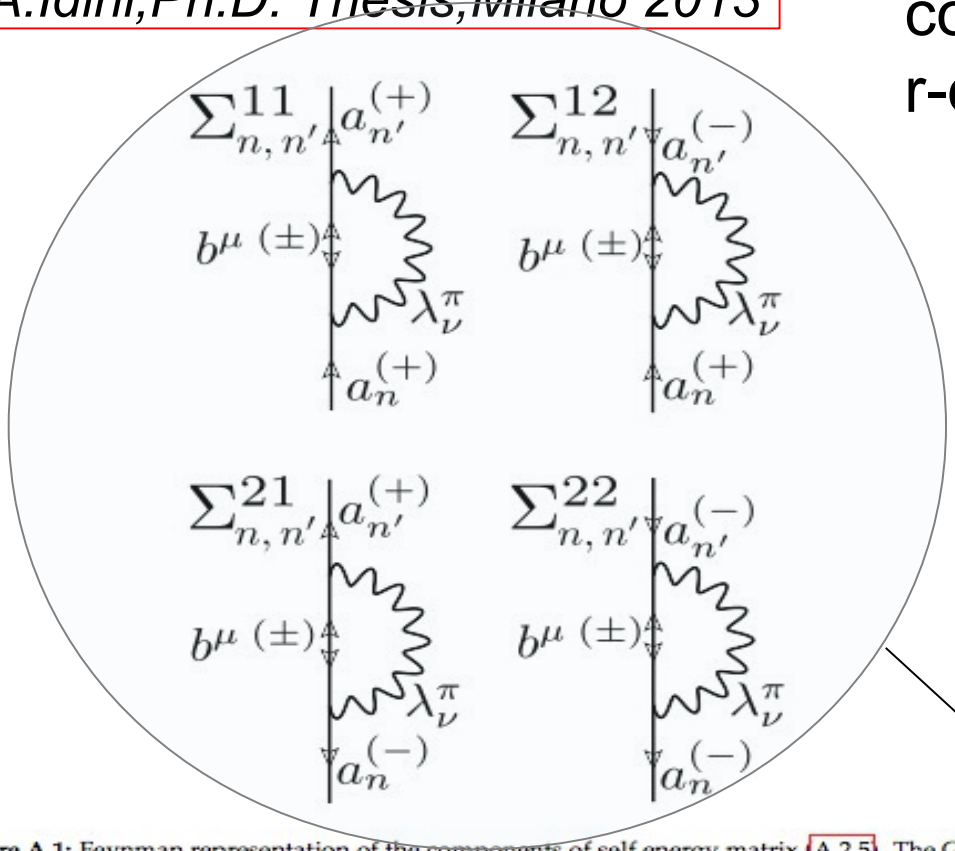

Figure A.1: Feynman representation of the components of self energy matrix (A.2.5). The Green's functions lines with the empty arrow represent respectively the positive and negative quasiparticle eigenvalue $^{(\pm)}$ of the basis (A.1.14)-(A.1.15).

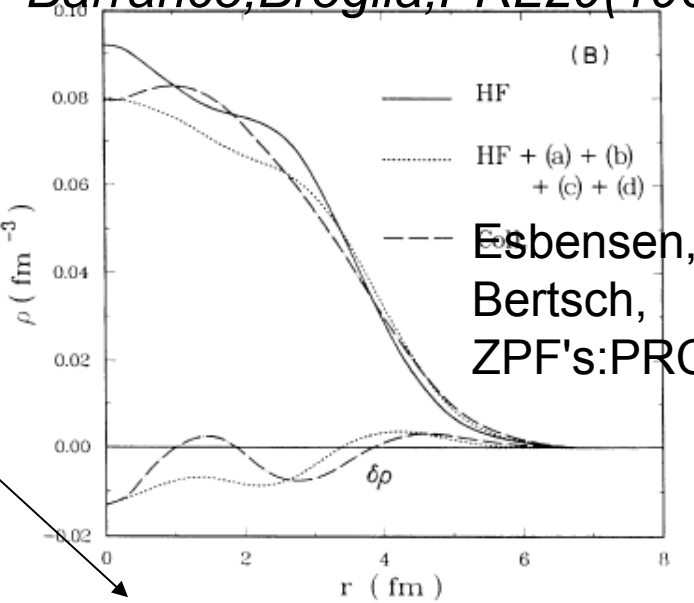

Esbensen, Bertsch, ZPF's:PRC28

$$\begin{pmatrix} -(\hat{T}+\hat{V}-\lambda)_{hh} & \hat{\Delta}^{t}_{ph} & -\Delta_{hh} & -(\hat{T}+\hat{V}-\lambda)_{hp} \\ \hat{\Delta}_{ph} & (\hat{T}+\hat{V}-\lambda)_{pp} & -(\hat{T}+\hat{V}-\lambda)_{ph} & \hat{\Delta}_{pp} \\ -\hat{\Delta}_{hh} & -(\hat{T}+\hat{V}-\lambda)_{hp} & (\hat{T}+\hat{V}-\lambda)_{hh} & -\hat{\Delta}_{hp} \\ -(\hat{T}+\hat{V}-\lambda)_{ph} & \hat{\Delta}^{t}_{pp} & -\Delta^{t}_{hp} & -(\hat{T}+\hat{V}-\lambda)_{pp} \end{pmatrix} + \begin{pmatrix} \Sigma^{11}_{hh} & \Sigma^{11}_{hp} & \Sigma^{12}_{hh} & \Sigma^{12}_{hp} \\ \Sigma^{11}_{ph} & \Sigma^{11}_{pp} & \Sigma^{12}_{ph} & \Sigma^{12}_{pp} \\ \Sigma^{21}_{hh} & \Sigma^{21}_{hp} & \Sigma^{22}_{hh} & \Sigma^{22}_{hp} \\ \Sigma^{21}_{ph} & \Sigma^{21}_{pp} & \Sigma^{22}_{ph} & \Sigma^{22}_{pp} \end{pmatrix}$$

Application to 10Li and 11Be: Talk by E. Vigezzi

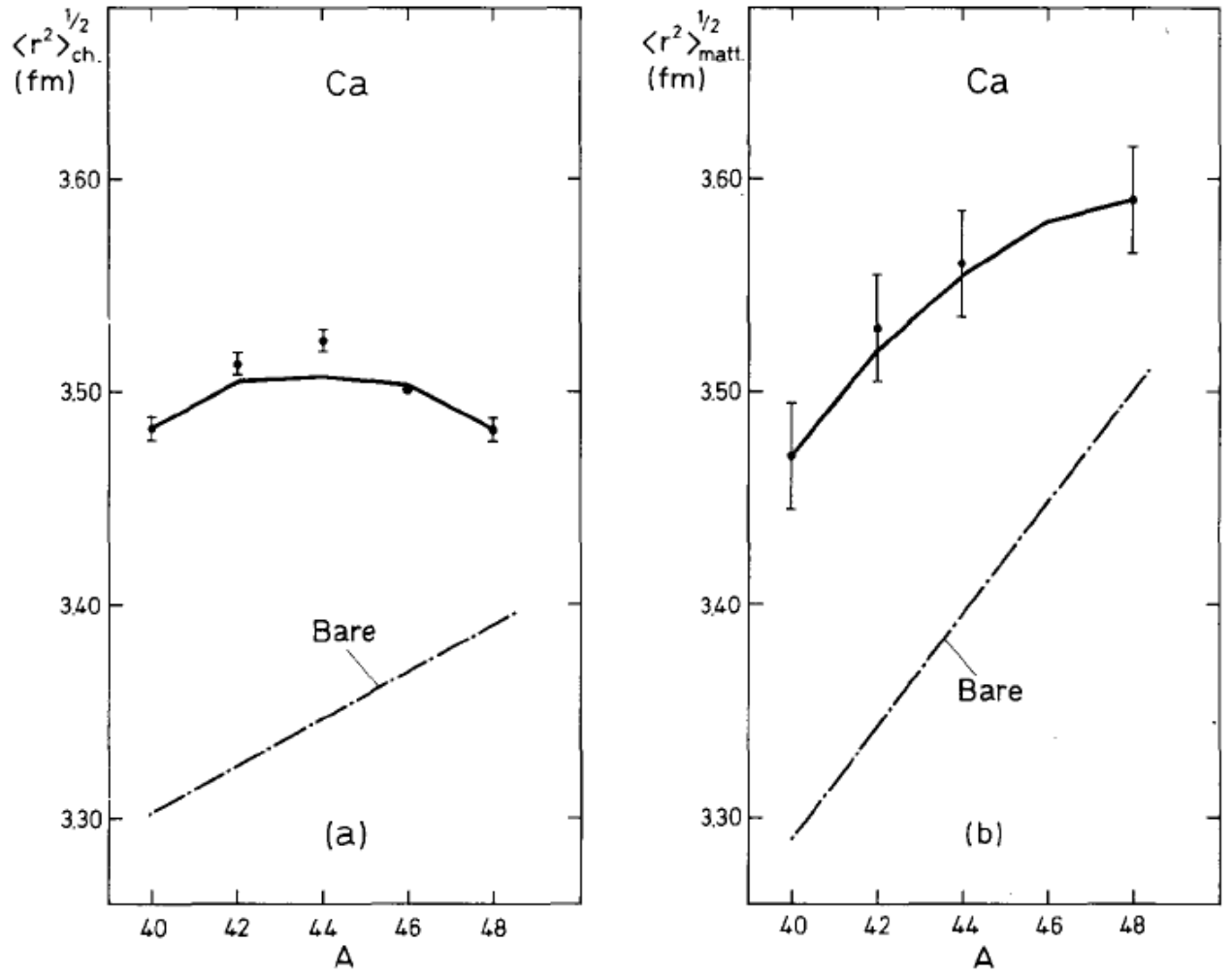

Fig. 1. Mean square radius of the Ca isotopes. In (a) the charge mean square radius is displayed as a function of the mass number [25–27]. The quantity $(\langle r^2 \rangle_0^{1/2})_{ch}$ was assumed to have a linear dependence with A. Its slope was fitted by requiring that the quantity (1) coincides with the experimental values for ^{40}Ca and ^{48}Ca making use of the values of $\Delta\sigma^2$ calculated through eqs. (2)–(4). These values are collected in table 1. The resulting values of $\langle r^2 \rangle_{ch}$ are displayed as a full drawn curve. In (b) the mass mean square radius is displayed [27]. The quantity $(\langle r^2 \rangle_0^{1/2})_{matt}$ was given an $A^{1/3}$ dependence, and its coefficient adjusted to get the best fit when use is made of eq. (1) and the quantities $\Delta\sigma^2$ (cf. table 1). The corresponding results are shown with a solid curve. The resulting bare mean square radius is $(\langle r^2 \rangle_0^{1/2})_{matt} = A^{1/3}\, 0.96$ fm.

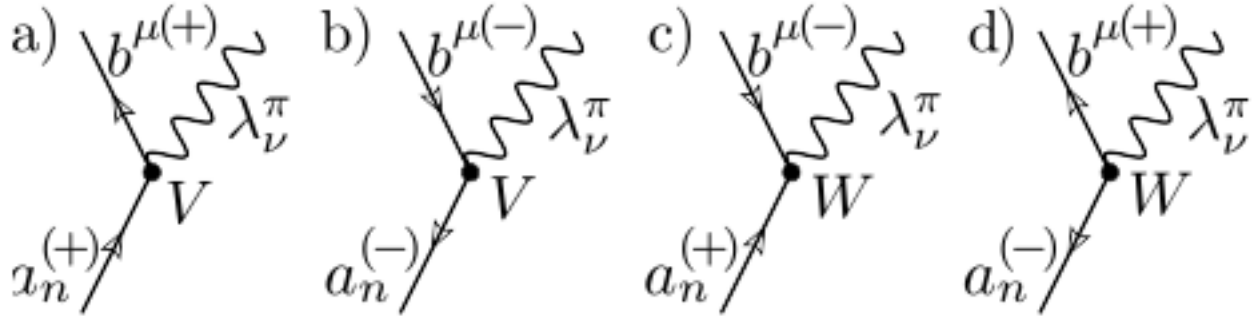

Figure A.2: Feynman representation of V and W vertices (A.2.8)-(A.2.11) for the case of particle a represented in the quasiparticle basis (A.1.14)-(A.1.15) $^{(\pm)}$ scattering into quasiparticle $b^{(\pm)}_{\mu}$ and a phonon λ^{π}_{ν}.

$$
\begin{aligned}
V(p_k^{(+)}, b^{\mu(+)}, \lambda_\nu^\pi) \equiv & \langle p_k^{(+)} | \hat{V_{res}} | b^{\mu(+)} \lambda_\nu^\pi \rangle = -\langle p_k^{(-)} | \hat{V_{res}} | b^{\mu(-)} \lambda_\nu^\pi \rangle \\
= & \langle 0 | a_{p_k} \hat{V_{res}} \alpha^\dagger_{b^\mu} \Gamma_{\lambda_\nu^\pi} | 0 \rangle = \langle 0 | a_{p_k} \hat{V} (\sum_l \widetilde{u}_{b^\mu,l} a^\dagger_{b_l} + \widetilde{v}_{b^\mu,l} a_{b_l}) \Gamma_{\lambda_\nu^\pi} | 0 \rangle \\
= & \sum_l (f+g)(p_k, b_l, \lambda_\nu^\pi) \widetilde{u}_{b^\mu,l} \qquad \text{cf. Fig. A.2(a)} \qquad (A.2.8) \\
V(h_k^{(+)}, b^{\mu(+)}, \lambda_\nu^\pi) \equiv & \langle h_k^{(+)} | \hat{V_{res}} | b^{\mu(+)} \lambda_\nu^\pi \rangle = -\langle h_k^{(-)} | \hat{V_{res}} | b^{\mu(-)} \lambda_\nu^\pi \rangle \\
= & \sum_l -\widetilde{v}_{b^\mu,l} (f-g)(h_k, b_l, \lambda_\nu^\pi) \qquad \text{cf. Fig. A.2(b),} \qquad (A.2.9) \\
W(p_k^{(+)}, b^{\mu(-)}, \lambda_\nu^\pi) \equiv & \langle p_k^{(+)} | \hat{V_{res}} | b^{\mu(-)} \lambda_\nu^\pi \rangle = \langle p_k^{(-)} | \hat{V_{res}} | b^{\mu(+)} \lambda_\nu^\pi \rangle \\
= & \sum_l \widetilde{v}_{b^\mu,l} (f-g)(p_k, b_l, \lambda_\nu^\pi) \qquad \text{cf. Fig. A.2(c),} \qquad (A.2.10) \\
W(h_k^{(+)}, b^{\mu(-)}, \lambda_\nu^\pi) \equiv & \langle h_k^{(+)} | \hat{V_{res}} | b^{\mu(-)} \lambda_n^\pi \rangle = \langle h_k^{(-)} | \hat{V_{res}} | b^{\mu(+)} \lambda_n^\pi \rangle \\
= & \sum_l \widetilde{u}_{b^\mu,l} (f+g)(h_k, b_l, \lambda_\nu^\pi) \qquad \text{cf. Fig. A.2(d).} \qquad (A.2.11)
\end{aligned}
$$

Similar developments (Soma,et.al,PRC87,011303(13)

Self-energy expansion

TECHNISCHE UNIVERSITÄT DARMSTADT

- Gorkov equations ⟶ energy *dependent* eigenvalue problem

$$\sum_b \begin{pmatrix} t_{ab} - \mu_{ab} + \Sigma^{11}_{ab}(\omega) & \Sigma^{12}_{ab}(\omega) \\ \Sigma^{21}_{ab}(\omega) & -t_{ab} + \mu_{ab} + \Sigma^{22}_{ab}(\omega) \end{pmatrix} \Bigg|_{\omega_k} \begin{pmatrix} \mathcal{U}^k_b \\ \mathcal{V}^k_b \end{pmatrix} = \omega_k \begin{pmatrix} \mathcal{U}^k_a \\ \mathcal{V}^k_a \end{pmatrix}$$

Ab Initio, and HF side, 2nd order

- 1st order ➟ energy-independent self-energy

$\Sigma^{11\,(1)}_{ab} =$ 

$\Sigma^{12\,(1)}_{ab} =$ 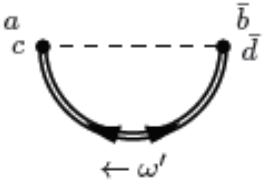

- 2nd order ➟ energy-dependent self-energy

$\Sigma^{11\,(2)}_{ab}(\omega) =$ 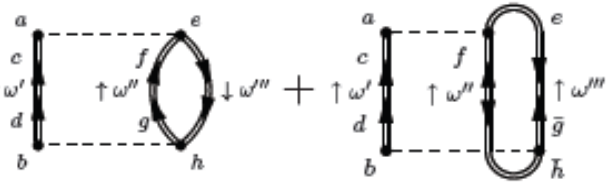

$\Sigma^{12\,(2)}_{ab}(\omega) =$ 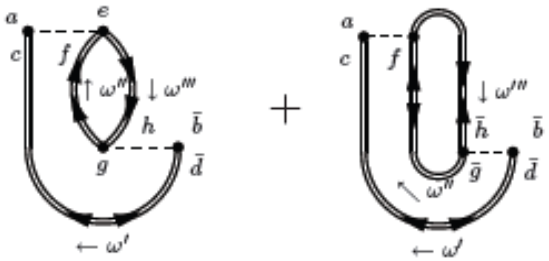

Scaling of Gorkov's problem

TECHNISCHE UNIVERSITÄT DARMSTADT

- Transformed into an energy *independent* eigenvalue problem

$$\begin{pmatrix} T-\mu+\Lambda & \tilde{h} & \mathcal{C} & -\mathcal{D}^\dagger \\ \tilde{h}^\dagger & -T+\mu-\Lambda & -\mathcal{D}^\dagger & \mathcal{C} \\ \mathcal{C}^\dagger & -\mathcal{D} & E & 0 \\ -\mathcal{D} & \mathcal{C}^\dagger & 0 & -E \end{pmatrix} \begin{pmatrix} \mathcal{U}^k \\ \mathcal{V}^k \\ \mathcal{W}_k \\ \mathcal{Z}_k \end{pmatrix} = \omega_k \begin{pmatrix} \mathcal{U}^k \\ \mathcal{V}^k \\ \mathcal{W}_k \\ \mathcal{Z}_k \end{pmatrix}$$

- Numerical scaling

$$m_{p,1} \approx \binom{N_b}{3} \propto \frac{N_b^3}{6}$$

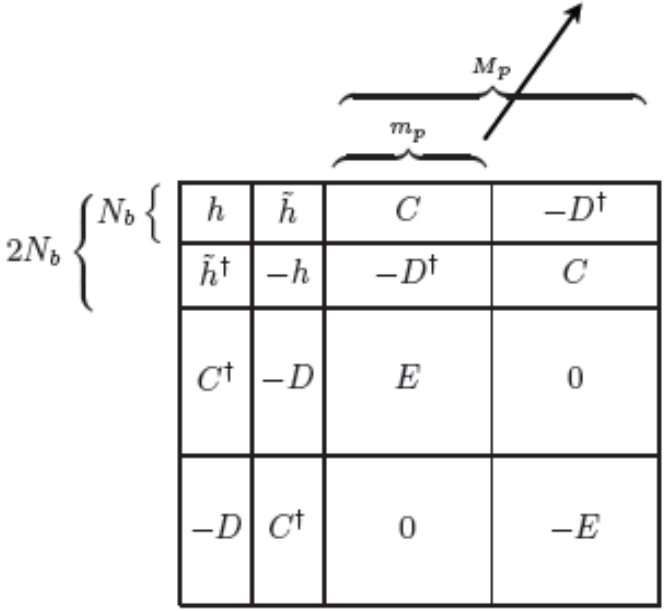

N_b → dimension of the s.p. basis

n → number of iterations

$$N_{tot,1} = 2N_b + M_{p,1} \approx N_b^3$$

$$\dots$$

$$N_{tot,n} = 2N_b + M_{p,n} \approx N_b^{3n}$$

Pairing gaps

TECHNISCHE UNIVERSITÄT DARMSTADT

- Three-point mass differences

$$\Delta_n^{(3)}(A) = \frac{(-1)^A}{2}[E_0^{A+1} - 2\,E_0^A + E_0^{A-1}]$$

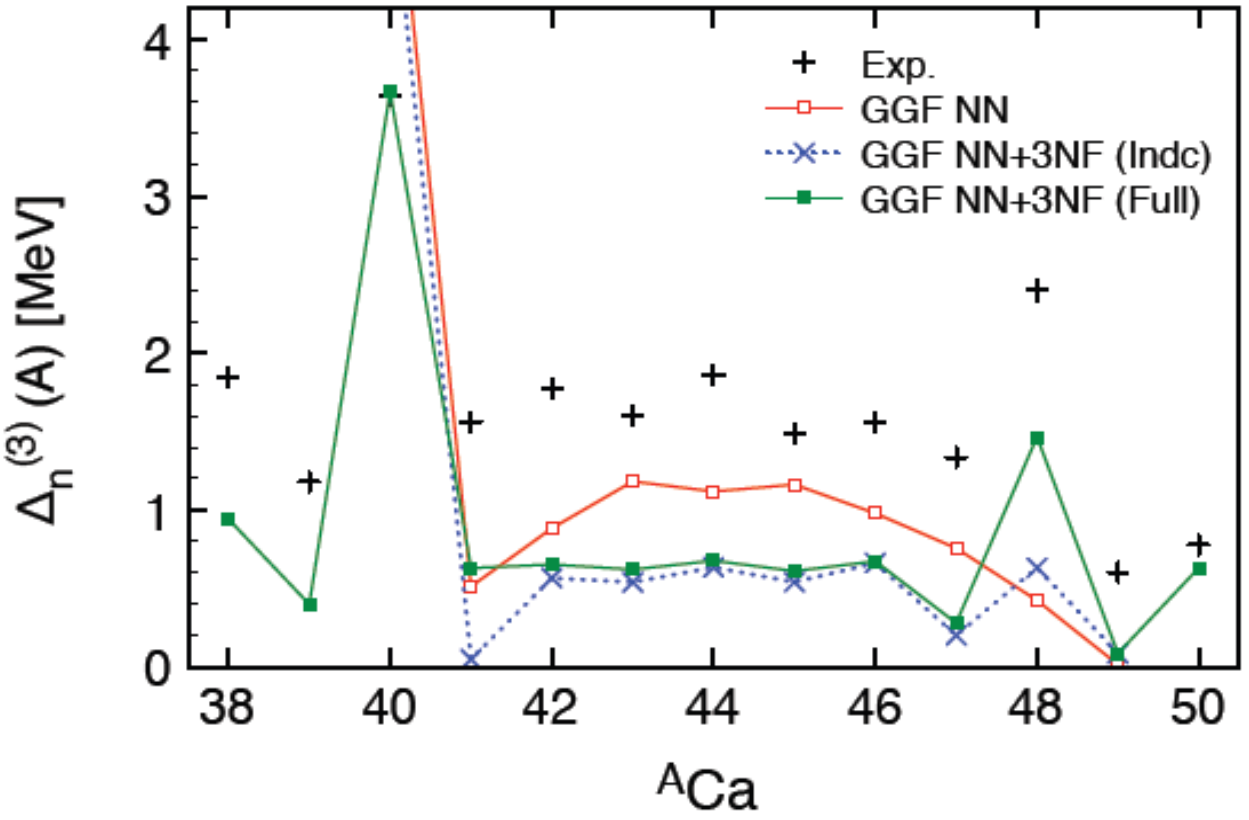

Shell Model Calculations

Holt, Menendez,Schwenk, arXiv1304.0434

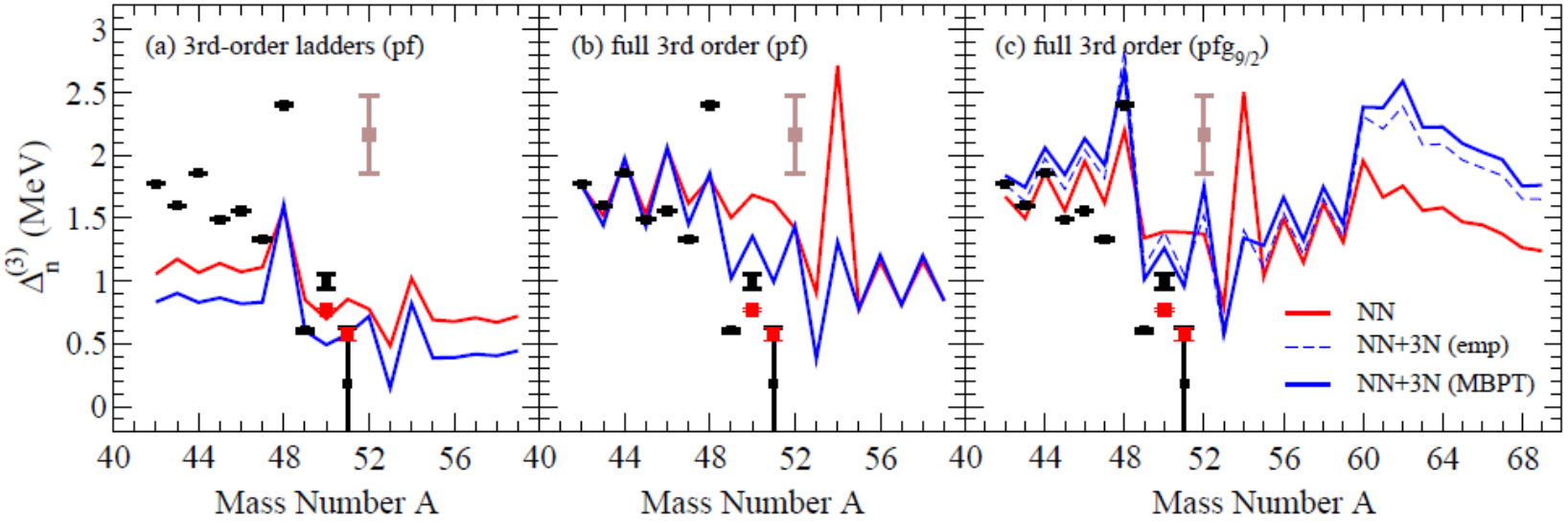

FIG. 3. (Color online) Three-point mass differences $\Delta_n^{(3)}$ in the calcium isotopes calculated to third order in MBPT with and without the leading chiral 3N forces, and in comparison with experiment [24, 67]. The legend is as in Fig. 1. Panel (a) shows the results of the third-order ladder contributions. Panels (b) and (c) include all MBPT diagrams to third order in the pf-shell and the extended $pfg_{9/2}$ valence space, respectively. The results in the pf-shell are with empirical SPEs. For the $pfg_{9/2}$ space, we show pairing gaps for both the MBPT and empirical SPEs.

When particle-hole contributions are included in a full third-order calculation, we find in Fig. 3 a clear improvement compared to including only ladder diagrams. In the pf-shell, the three-point mass differences are increased, leading to reasonable agreement with experimental data. This clearly demonstrates the importance of particle-hole many-body processes, such as core-polarization, on pairing in nuclei. Our results show that they can provide the missing pairing strength required to reproduce experiment on top of the direct NN+3N interactions. Analogously, the systematic differences between theoretical and experimental pairing gaps found in the EDF approach of Ref. [15] may be attributed to these effects.

Fadeev RPA,
Barbieri,Dickhoff;PRC63,034313(2001)

C. BARBIERI AND B. K. JENNINGS PRC72,014613(2005)

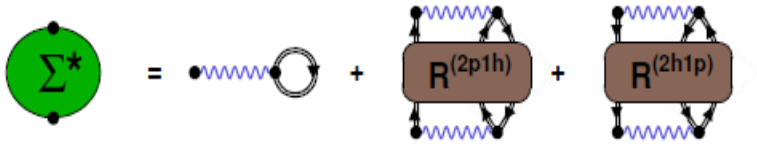

FIG. 1. (Color online) Feynman diagrams representation of the self energy. The first diagram on the right-hand side represents the Hartree-Fock–like contribution to the mean field. The remaining ones describe core polarization effects in the particle (2p1h) and hole (2h1p) part of the spectrum.

Combines
i)particle,
ii)ph-RPA and
iii)pp(hh)-RPA
consistently

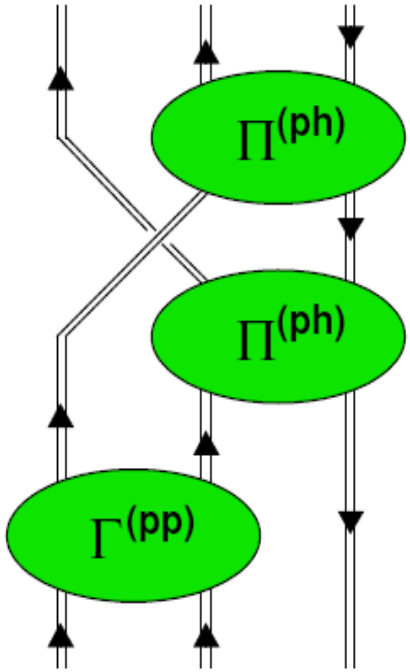

FIG. 2. (Color online) Example of a diagrammatic contribution included in the Faddeev expansion for $R^{(2p1h)}$ (see Fig. 1). A quasiparticle is coupled to the response function $\Pi^{(ph)}$ that describes the target nucleus. It can also participate in pairing processes, which are accounted for by the two-body propagator $g^{II,(pp)}$.

CONCLUSIONS

a. At mean field level surface pairing interaction prefered.
Bare Argonne tractable as pairing interaction.

b. Phonon Exchange Pairing Induced Interaction very
surface peaked. In volumen could be repulsive due
to spin modes.
Strong A-dependence from the Slab Model.

c. Close connection to self-energy effects from
Dyson Gorkov's eqs.: Quasi-particle Phonon Coupling:
Fragmentation and Dense Espectra<=> Induced Pairing Int.
Bare Argonne plus Induced Pairing good description of data.

d. Shell Model confirms relevance of surface phonons mediated
pairing interaction.

e. Multishell Self-energy: Full HFB renormalization.
Ab Initio calculations in progress (2^{nd} order).